Creep and Shrinkage Prediction Model for Analysis and Design of Concrete Structures: Model B3

By Zdeněk P. Bažant and Sandeep Baweja

SYNOPSIS: The present paper[*] presents in chapter 1 a model for the characterization of concrete creep and shrinkage in design of concrete structures (Model B3), which is simpler, agrees better with the experimental data and is better theoretically justified than the previous models. The model complies with the general guidelines recently formulated by RILEM TC-107ß1. Justifications of various aspects of the model and diverse refinements are given in Chapter 2, and many simple explanations are appended in the commentary at the end of Chapter 1 (these parts do not to be read by those who merely want to apply the model). The prediction model B3 is calibrated by a computerized data bank comprising practically all the relevant test data obtained in various laboratories throughout the world. The coefficients of variation of the deviations of the model from the data are distinctly smaller than those for the latest CEB model (1990), and much smaller than those for the previous model in ACI 209 (which was developed in the mid-1960's). The model is simpler than the previous models (BP and BP-KX) developed at Northwestern University, yet it has comparable accuracy and is more rational. The effect of concrete composition and design strength on the model parameters is the main source of error of the model. A method to reduce this error by updating one or two model parameters on the basis of short-time creep tests is given. The updating of model parameters is particularly important for high-strength concretes and other special concretes containing various admixtures, superplasticizers, water-reducing agents and pozzolanic materials. For the updating of shrinkage prediction, a new method in which the shrinkage half-time is calibrated by simultaneous measurements of water loss is presented. This approach circumvents the large sensitivity of the shrinkage extrapolation problem to small changes in the material parameters. The new model allows a more realistic assessment of the creep and shrinkage effects in concrete structures, which significantly affect the durability and long-time serviceability of civil engineering infrastructure.

Zdeněk P. Bažant, F.ACI, was born and educated in Prague (Ph.D. 1963). He joined Northwestern University faculty in 1969, became Professor in 1973, was named to the distinguished W.P. Murphy Chair in 1990, and served during 1981-87 as Director of the Center for Concrete and Geomaterials. In 1996 he was elected to the *National Academy of Engineering*. He has authored almost 400 refereed journal articles and published books on *Stability of Structures* (1991), *Fracture and Size Effect* (1997), *Concrete at High Temperatures* (1996) and *Creep of Concrete* (1966). He served as *Editor* (in chief) of ASCE J. of Engrg. Mech. (1988-94) and is Regional Editor of Int. J. of Fracture. He was founding president of IA-FraMCoS, president of Soc. of Engrg. Science (SES), and chairman of SMiRT Div. H. He is an Illinois Registered Structural Engineer, and chaired various techn. committees in ASCE, RILEM and ACI. His honors include: *Prager Medal* from SES; Warner Medal from ASME, *Newmark Medal, Croes Medal* and *Huber Prize* and *T.Y. Lin Award* from ASCE; *L'Hermite Medal* from RILEM; *Humboldt Award*; *Honorary Doctorates* from ČVUT, Prague, and from Universität Karlsruhe; *Guggenheim, NATO, JSPS, Ford and Kajima Fellowships*; etc. He is a Foreign Member of Academy of Engrg. of Czech Rep. and a *fellow* of Am. Academy of Mechanics, ASME, ASCE and RILEM.

Sandeep Baweja, M.ACI, earned a Ph.D. in structural engineering from Northwestern University in 1996. He is now a Senior Software Engineer at EA Systems, Inc., Alameda, California, and serves as a member of ACI Committee 209, Creep and Shrinkage. His research interests include constitutive modeling of structural materials, especially concrete, computational mechanics, and computer aided engineering.

Chapter 1

Description of Model B3 and Prediction Procedure

1.1 Introduction

During the last two decades, significant advances in the understanding of creep and shrinkage of concrete have been achieved. They include: (1) vast expansion of the experimental data base on concrete creep and shrinkage; (2) compilation of a computerized data bank; (3) development of computerized statistical procedures for data fitting and optimization; and (4) improved understanding of the physical processes involved in creep and shrinkage, such as the aging, diffusion processes, thermally activated processes, microcracking and their mathematical modeling. These advances have made possible the formulation of the present model, which represents an improvement compared to the model in ACI 209. The new model (representing the third major updateß2 of the modelsß3,4 developed at Northwestern University) is labeled Model B3.

In Chapter 1 of this paper, the model is formulated succinctly, without any explanations, justifications, extensions and refinements. These are relegated to Chapter 2 and to the Commentary at the end of Chapter 1 of this report, which does not have to be read by those who merely want to apply the model and do not have time for curiosity about its justification. The methods and typical examples of structural analysis for creep and shrinkage will not be discussed in this report because they are adequately treated in Chapters 3-5 of ACI 209 as well as some books.

A background at the level of standard undergraduate courses in mechanics of materials, structural mechanics, engineering mathematics and concrete technology is expected from the user.

The present model represents an improved alternative to Chapter 2 of ACI 209. Chapters 3-5 of that report, dealing with the structural response, remain applicable to the present report. The improvement means that the coefficient of variation of the errors of the predictions of creep and shrinkage strains are 23 % for creep (basic and with drying) and 34% for shrinkage for the present model, while those for the model from Chapter 2 of ACI 209 are

58% for basic creep, 45% for creep with drying and 55% for shrinkage. The penalty is some reduction in simplicity of the model. The user should decide what accuracy he needs depending on the sensitivity of the structure defined in Section 1.2.1

1.2   Applicability Range

1.2.1   Levels of Creep Sensitivity of Structures and Type of Analysis Required

Accurate and laborious analysis of creep and shrinkage is necessary only for some special types of structures. That depends on the sensitivity of the structure. Although more precise studies are needed, the following approximate classification of sensitivity levels of structures can be made on the basis of general experience[C1,*].

Level 1. Reinforced concrete beams, frames and slabs with spans under 65 ft (20 m) and heights of up to 100 ft (30 m), plain concrete footings, retaining walls.

Level 2. Prestressed beams or slabs of spans up to 65 ft. (20 m), high-rise building frames up to 325 ft (100 m) high.

Level 3. Medium-span box girder, cable-stayed or arch bridges with spans of up to 260 ft (80 m), ordinary tanks, silos, pavements.

Level 4. Long-span prestressed box girder, cable-stayed or arch bridges; large bridges built sequentially in stages by joining parts; large gravity, arch or buttress dams; cooling towers; large roof shells; very tall buildings.

Level 5. Record span bridges, nuclear containments and vessels, large off-shore structures, large cooling towers, record-span thin roof shells, record-span slender arch bridges.

The foregoing grouping of structures is only approximate. If in doubt to which level a given structure belongs one should undertake an accurate analysis of the creep and shrinkage effects in a given structure (such as maximum deflection, change of maximum stress and crack width) and then judge the severity of the effects compared to those of the applied loads.

The model presented in this report is necessary for levels 4 and 5. It is also preferable but not necessary for level 3. For level 2 and as an acceptable approximation also for level 3, simpler models are adequate including the model in Chapter 2 of ACI 209.

A refined model such as that presented here ought to be always used for structures analyzed by sophisticated computer methods, particularly the finite element method (because it makes no sense to input inaccurate material properties into a very accurate computer program). The error in maximum

---

*Superscripts preceded by 'C' refer to the comments listed in the Commentary in Section 1.7.8

4

deflections or stresses caused by replacing an accurate analysis of creep and shrinkage effects with a simple but crude estimation is often larger than the gain from replacing old fashioned frame analysis by hand with a computer analysis by finite elements.

The age-adjusted effective modulus method (ACI 209) is recommended for levels 3 and 4. The effective modulus method suffices for level 2. For level 1, creep and shrinkage analysis of the structure is not needed but a crude empirically based estimate is desirable. Level 5 requires the most realistic and accurate analysis possible, typically a step-by-step computer solution based on a general constitutive law, coupled with the solution of the differential equations for drying and heat conduction.

The creep and shrinkage deformations invariably exhibit large statistical scatter. Therefore a statistical analysis with estimation of 95% confidence limits is mandatory for level 5. It is highly recommended for level 4. For lower levels it is desirable but not necessary, however, the confidence limits for any response X (such as deflection or stress) should be considered, being estimated $\bar{X} \times (1 \pm 1.96\omega)$ where $\bar{X}$ = mean estimate of X and ω is taken same as in Eq. (1.25).

Analysis of temperature effects and effects of cycling of loads and environment ought to be detailed for level 5 and approximate for level 4. It is not necessary though advisable for level 3 and can be ignored for levels 1 and 2 (except perhaps for the heat of hydration effects).

1.2.2   Parameter Ranges

The prediction of the material parameters of the present model from strength and composition is restricted to Portland cement concrete with the following parameter ranges:[C2]

$$0.35 \leq w/c \leq 0.85, \quad 2.5 \leq a/c \leq 13.5 \tag{1.1}$$

$$
\begin{array}{llll}
2500 \text{ psi} \leq \bar{f}_c \leq 10,000 \text{ psi}, & 10 \text{ lb/ft}^3 \leq c \leq 45 \text{ lbs/ft}^3 & \text{inch-pound system} \\
17 \text{ MPa} \leq \bar{f}_c \leq 70 \text{ MPa} & 160 \text{ kg/m}^3 \leq c \leq 720 \text{ kg/m}^3 & \text{SI}
\end{array}
\tag{1.2}
$$

$\bar{f}_c$ is the 28 day standard cylinder compression strength of concrete (in psi (inch-pound system) or MPa (SI) units), w/c is the water-cement ratio by weight, c is the cement content (in lb/ft^3 (inch-pound system) or kg/m^3 (SI) units) and a/c is the aggregate-cement ratio by weight. The formulae are valid for concretes cured for at least one day[C3].

1.3   Definitions, Basic Concepts and Overview of Calculation Procedures

The present prediction model is restricted to the service stress range[C4] (or up to about $0.45\bar{f}_c$, where $\bar{f}_c$ = mean cylinder strength at 28 days). This

means that, for constant stress applied at age t',

$$\epsilon(t) = J(t, t')\sigma + \epsilon_{sh}(t) + \alpha \Delta T(t) \tag{1.3}$$

in which $J(t, t')$ is the compliance function = strain (creep plus elastic) at time t caused by a unit uniaxial constant stress[C5,C6] applied at age t', σ = uniaxial stress , ϵ = strain (both σ and ϵ are positive if tensile), ϵ_{sh} = shrinkage strain (negative if volume decreases) $\Delta T(t)$ = temperature change from reference temperature at time t, and α = thermal expansion coefficient (which may be approximately predicted according to ACI 209ß5).

The compliance function may further be decomposed as

$$J(t, t') = q_1 + C_0(t, t') + C_d(t, t', t_0) \tag{1.4}$$

in which q_1 = instantaneous strain due to unit stress, $C_0(t, t')$ = compliance function for basic creep (creep at constant moisture content and no moisture movement through the material), and $C_d(t, t', t_0)$ = additional compliance function due to simultaneous drying[C7].

The creep coefficient, $\phi(t, t')$, which represents the most convenient way to introduce creep into structural analysis, should be calculated from the compliance function[C8]:

$$\phi(t, t') = E(t')J(t, t') - 1 \tag{1.5}$$

where $E(t')$ = (static) modulus of elasticity at loading age t'.

The relative humidity in the pores of concrete is initially 100%. In the absence of moisture exchange (as in sealed concrete), a gradual decrease of pore humidity, called self-desiccation, is caused by hydration[C9]. Exposure to the environment engenders a long-term drying process (described by the solution of the diffusion equation), which causes shrinkage and additional creep[C10]. In the absence of drying there is another kind of shrinkage, called autogeneous shrinkage, which is caused by the chemical reactions of hydration. This shrinkage is usually small for normal concretes (not for high-strength concretes) and can usually be neglected[C11].

In the following sections, first the expressions for the individual terms in Eq. (1.3)–(1.4)will be presented. The formulae to predict the coefficients of these equations, statistically derived from calibration with the data bank, will be given next. Two examples of the calculation procedure will then be given. Estimation of the statistical scatter of the predicted shrinkage and creep values due to parameter uncertainties will be discussed next. Finally, a method of improving the predictions of the model by extrapolation of short-time test data will be presented.

1.4 Calculations of Creep and Time Dependent Strain Components

1.4.1 Basic Creep (Material Constitutive Property)

The basic creep compliance is more conveniently defined by its time rate than its value:

$$\dot{C}_0(t, t') = \frac{n(q_2 t^{-m} + q_3)}{(t - t') + (t - t')^{1-n}} + \frac{q_4}{t}, \qquad m = 0.5, n = 0.1 \qquad (1.6)$$

in which $\dot{C}_0(t, t') = \partial C_0(t, t')/\partial t$, t and t' must be in days, m and n are empirical parameters whose value can be taken the same for all normal concretes and are indicated above; and q_2, q_3 and q_4 are empirical constitutive parameters which will be defined later[C12]. The total basic creep compliance is obtained by integrating Eq. (1.6)as follows:

$$C_0(t, t') = q_2 Q(t, t') + q_3 \ln[1 + (t - t')^n] + q_4 \ln\left(\frac{t}{t'}\right) \qquad (1.7)$$

in which $Q(t, t')$ is given in Table 1.1 and can also be calculated from an approximate explicit formula given by Eq. (1.35) in the Appendix to Chapter 1^{C13}. Function $Q(t, t')$, of course, can also be easily obtained by numerical integration (see Section 1.8.1 in the Appendix).

Table 1.1: Values of function $Q(t, t')$ for $m = 0.5$ and $n = 0.1$

| log (t-t') | log t' | | | | | | | | |
	0.0	0.5	1.0	1.5	2.0	2.5	3.0	3.5	4.0
-2.0	0.4890	0.2750	0.1547	0.08677	0.04892	0.02751	0.01547	0.008699	0.004892
-1.5	0.5347	0.3009	0.1693	0.09519	0.05353	0.03010	0.01693	0.009519	0.005353
-1.0	0.5586	0.3284	0.1848	0.1040	0.05846	0.03288	0.01849	0.01040	0.005846
-0.5	0.6309	0.3571	0.2013	0.1133	0.06372	0.03583	0.02015	0.01133	0.006372
0.0	0.6754	0.3860	0.2185	0.1231	0.06929	0.03897	0.02192	0.01233	0.006931
0.5	0.7108	0.4125	0.2357	0.1334	0.07516	0.04229	0.02379	0.01338	0.007524
1.0	0.7352	0.4335	0.2514	0.1436	0.08123	0.04578	0.02576	0.01449	0.008149
1.5	0.7505	0.4480	0.2638	0.1529	0.08727	0.04397	0.02782	0.01566	0.008806
2.0	0.7597	0.4570	0.2724	0.1602	0.09276	0.05239	0.02994	0.01687	0.009494
2.5	0.7652	0.4624	0.2777	0.1652	0.09708	0.05616	0.03284	0.01812	0.01021
3.0	0.7684	0.4656	0.2808	0.1683	0.1000	0.05869	0.03393	0.01935	0.01094
3.5	0.7703	0.4675	0.2827	0.1702	0.1018	0.06041	0.03541	0.02045	0.01166
4.0	0.7714	0.4686	0.2838	0.1713	0.1029	0.06147	0.03641	0.02131	0.01230
4.5	0.7720	0.4692	0.2844	0.1719	0.1036	0.06210	0.03702	0.02190	0.01280
5.0	0.7724	0.4696	0.2848	0.1723	0.1038	0.06247	0.03739	0.02225	0.01314

The terms in Eq. (1.7) containing q_2, q_3 and q_4 represent the aging viscoelastic compliance, non-aging viscoelastic compliance, and flow compliance, respectively, as deduced from the solidification theoryß6.

1.4.2 Average Shrinkage and Creep of Cross Section at Drying

Shrinkage

Mean shrinkage strain in the cross section:

$$\epsilon_{sh}(t, t_0) = -\epsilon_{sh\infty} \, k_h \, S(t) \tag{1.8}$$

Time dependence:

$$S(t) = \tanh\sqrt{\frac{t - t_0}{\tau_{sh}}} \tag{1.9}$$

Humidity dependence:

$$k_h = \begin{cases} 1 - h^3 & \text{for} & h \leq 0.98 \\ -0.2 & \text{for} & h = 1 \text{ (swelling in water)} \\ \text{linear interpolation} & \text{for} & 0.98 \leq h \leq 1 \end{cases} \tag{1.10}$$

Size dependence:

$$\tau_{sh} = k_t (k_s D)^2 \tag{1.11}$$

where v/s = volume to surface ratio of the concrete member, $D = 2v/s$ = effective cross-section thickness which coincides with the actual thickness in the case of a slab, k_t is a factor defined by Eq. (1.20) and k_s is the cross-section shape factor:

$$k_s = \begin{cases} 1.00 & \text{for} & \text{an infinite slab} \\ 1.15 & \text{for} & \text{an infinite cylinder} \\ 1.25 & \text{for} & \text{an infinite square prism} \\ 1.30 & \text{for} & \text{a sphere} \\ 1.55 & \text{for} & \text{a cube} \end{cases} \tag{1.12}$$

The analyst needs to estimate which of these shapes best approximates the real shape of the member or structure. High accuracy in this respect is not needed and $k_s \approx 1$ can be assumed for simplified analysis.

Time-dependence of ultimate shrinkage:

$$\epsilon_{sh\infty} = \epsilon_{s\infty} \frac{E(607)}{E(t_0 + \tau_{sh})}; \qquad E(t) = E(28) \left(\frac{t}{4 + 0.85t} \right)^{1/2} \tag{1.13}$$

where $\epsilon_{s\infty}$ is a constant (given by Eq. 1.19). This means that $\epsilon_{s\infty} = \epsilon_{sh\infty}$ for $t_0 = 7$ days and $\tau_{sh} = 600$ days[C14].

Additional Creep Due to Drying (Drying Creep)

$$C_d(t, t', t_0) = q_5 \left[\exp\{-8H(t)\} - \exp\{-8H(t'_0)\} \right]^{1/2}, \quad t'_0 = \max(t', t_0) \tag{1.14}$$

if $t \geq t'_0$, otherwise $C_d(t, t', t_0) = 0$; t'_0 is the time at which drying and loading first act simultaneously; and

$$H(t) = 1 - (1 - h)S(t) \tag{1.15}$$

Fig. 1.1 shows the typical curves of basic creep, shrinkage and drying creep according to the present model.

1.4.3   Prediction of Model Parameters

Some formulae that follow are valid only in certain dimensions. Those are given both in inch-pound system units (psi, in.) and in SI (metric) units (MPa, m). The units of each dimensional quantity are also specified in the list of notations (Appendix to Chapter 1)[C15].
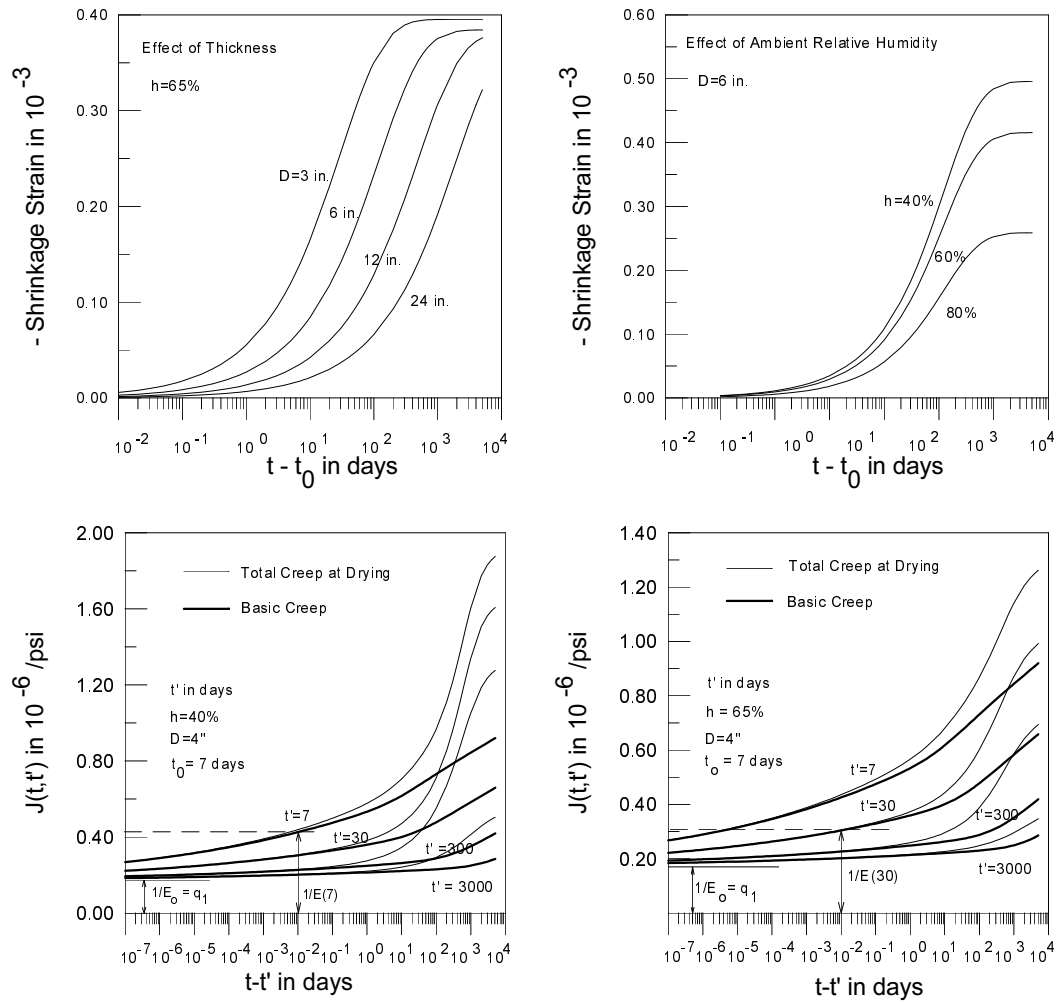
Top-left plot:

- Shrinkage Strain in 10^{-3} (y-axis)

Effect of Thickness

h=65%

D=3 in.
6 in.
12 in.
24 in.

$t - t_0$ in days (x-axis): 10^{-2} 10^{-1} 10^0 10^1 10^2 10^3 10^4

Top-right plot:

- Shrinkage Strain in 10^{-3} (y-axis)

Effect of Ambient Relative Humidity

D=6 in.

h=40%
60%
80%

$t - t_0$ in days (x-axis): 10^{-2} 10^{-1} 10^0 10^1 10^2 10^3 10^4

Bottom-left plot:

$J(t,t')$ in 10^{-6}/psi (y-axis)

Total Creep at Drying
Basic Creep

t' in days
h=40%
D=4"
t_0= 7 days

t'=7
t'=30
t' =300
t' = 3000

$1/E_o = q_1$
$1/E(7)$

t-t' in days (x-axis): 10^{-7} 10^{-6} 10^{-5} 10^{-4} 10^{-3} 10^{-2} 10^{-1} 10^0 10^1 10^2 10^3 10^4

Bottom-right plot:

$J(t,t')$ in 10^{-6}/psi (y-axis)

Total Creep at Drying
Basic Creep

t' in days
h = 65%
D=4"
t_o = 7 days

t'=7
t'=30
t'=300
t'=3000

$1/E_o = q_1$
$1/E(30)$

t-t' in days (x-axis): 10^{-7} 10^{-6} 10^{-5} 10^{-4} 10^{-3} 10^{-2} 10^{-1} 10^0 10^1 10^2 10^3 10^4

Figure 1.1: Typical creep and shrinkage curves given by Model B3

1.4.4 Estimation from Concrete Strength and Composition

Basic Creep

$$q_1 = 0.6 \times 10^6/E_{28}, \qquad E_{28} = 57000\sqrt{\bar{f}_c} \qquad \text{inch-pound system}$$
$$q_1 = 0.6 \times 10^6/E_{28}, \qquad\qquad E_{28} = 4734\sqrt{\bar{f}_c} \qquad \text{SI} \tag{1.16}$$

$$q_2 = 451.1 c^{0.5}\bar{f}_c^{-0.9}, \quad q_4 = 0.14(a/c)^{-0.7} \quad \text{inch-pound system}$$
$$q_2 = 185.4 c^{0.5}\bar{f}_c^{-0.9}, \quad q_4 = 20.3(a/c)^{-0.7} \qquad \text{SI} \tag{1.17}$$

$$q_3 = 0.29(w/c)^4 q_2 \tag{1.18}$$

Shrinkage

$$\epsilon_{s\infty} = -\alpha_1\alpha_2\left[26 w^{2.1}\bar{f}_c^{-0.28} + 270\right] \qquad (\text{in } 10^{-6}) \qquad \text{inch-pound system}$$
$$\epsilon_{s\infty} = -\alpha_1\alpha_2\left[1.9 \times 10^{-2} w^{2.1}\bar{f}_c^{-0.28} + 270\right] \qquad (\text{in } 10^{-6}) \qquad \text{SI} \tag{1.19}$$

and

$$k_t = 190.8 t_0^{-0.08}\bar{f}_c^{-1/4} \text{ days/in}^2 \quad \text{inch-pound system}$$
$$k_t = 8.5 t_0^{-0.08}\bar{f}_c^{-1/4} \text{ days/cm}^2 \qquad \text{SI} \tag{1.20}$$

where

$$\alpha_1 = \begin{cases} 1.0 & \text{for type I cement;} \\ 0.85 & \text{for type II cement;} \\ 1.1 & \text{for type III cement.} \end{cases} \tag{1.21}$$

and

$$\alpha_2 = \begin{cases} 0.75 & \text{for steam-curing;} \\ 1.2 & \text{for sealed or normal curing in air with initial protection against drying;} \\ 1.0 & \text{for curing in water or at 100\% relative humidity.} \end{cases} \tag{1.22}$$

Creep at Drying (same in both inch-pound system and SI units)

$$q_5 = 7.57 \times 10^5 \bar{f}_c^{-1} \mid \epsilon_{sh\infty} \mid^{-0.6} \tag{1.23}$$

1.4.5 Example of Calculation of Model B3

The user may check the correctness of his implementation of Model B3 by a comparison with the following example. This example is based on the test data from Ref. 7. Calculations are made with four digit accuracy so that the user may dependably check his program, even though such accuracy is not justified by tests.[†]

Given concrete properties: 1) Type I cement concrete; 2) age of concrete $t = 112$ days; 3) age at loading $t' = 28$ days; 4) age when drying begins $t_0 =$

[†]This example was prepared by A. Al-Manaseer and T. Monawar, Department of Civil Engineering and Construction, Bradley University.

28 days; 5) relative humidity $h = 100\%$; 6) cylinder compression strength $\bar{f}_c = 4000$ psi; 7) volume to surface ratio $v/s = 0.75$; 8) cement content $c = 13.69$ lb/ft^3; 9) water-cement ratio $w/c = 0.60$; 10) water content of concrete $w = 8.23$ lb/ft^3; 11) aggregate-cement ratio $a/c = 7.0$; 12) applied stress (40 % of $\bar{f}_c$) $\sigma = 1600$ psi.

Compliance function: $J(t, t') = q_1 + C_0(t, t') + C_d(t, t', t_0)$ (Eq. 1.4)

$q_1 = 0.6 \times 10^6/E_{28}$ (Eq. 1.16)

$E_{28} = 57000(\bar{f}_c)^{0.5} = 57000 \times (4000)^{0.5} = 3,605,000$ psi   (Eq. 1.16)

$q_1 = 0.6 \times 10^6/3,605,000 = 0.1664$

$C_0(t, t') = q_2 Q(t, t') + q_3 \ln[1 + (t - t')^n] + q_4 \ln(t/t')$ (Eq. 1.7)

$q_2 = 451.1c^{0.5}(\bar{f}_c)^{-0.9} = 451.1 \times 13.69^{0.5} \times 4000^{-0.9} = 0.9564$ (Eq. 1.17)

$q_3 = 0.29(w/c)^4 q_2 = 0.29 \times 0.6^4 \times 0.9564 = 0.0359$ (Eq. 1.18)

$r(t') = 1.7(t')^{0.12} + 8 = 1.7 \times 28^{0.12} + 8 = 10.5358$ (Eq. 1.36)

By interpolation from Table 1.1^{C16}: $Q(t, t') = 0.1681$

$C_0(t, t') = 0.9564 \times 0.1681 + 0.0359 \times \ln[1 + (112 - 28)^{0.1}] + 0.0359 \ln(112/28) = 0.2443$

$C_d(t, t', t_0) = q_5[\exp\{-8H(t)\} - \exp\{-8H(t')\}]^{1/2}$ (Eq. 1.14)

$\alpha_1 = 1.0$, $\alpha_2 = 1.0$ (Eq. 1.21–1.22)

$\epsilon_{s\infty} = \alpha_1 \alpha_2[26w^{2.1}(\bar{f}_c)^{-0.28} + 270] = 1.0 \times 1.0 \times [26 \times 8.23^{2.1} \times 4000^{-0.28} + 270] = 483.1749 \approx \epsilon_{sh\infty}$ (Eq. 1.19)

$q_5 = 7.57 \times 10^5(\bar{f}_c)^{-1}ABS(\epsilon_{s\infty})^{-0.6} = 4.6406$ (Eq. 1.23)

$k_s = 1.00$ (Eq. 1.12)

$k_t = 190.8t_0^{-0.08}\bar{f}_c^{-1/4} = 18.3777$ (Eq. 1.20)

$\tau_{sh} = k_t(k_s D)^2 = 41.3498$ (Eq. 1.11)

$S(t) = \tanh[(t - t_0)/\tau_{sh}]^{0.5} = 0.8907$ (Eq. 1.9)

$S(t') = \tanh[(t' - t_0)/\tau_{sh}]^{0.5} = 0.0$

$H(t) = 1 - (1 - h)S(t) = 1 - (1 - 1) \times 0.8907 = 1$ (Eq. 1.15)

$H(t') = 1 - (1 - h)S(t') = 1 - (1 - 1) \times 0.0 = 1$

$C_d(t, t', t_0) = 4.6406 \times [\exp(0.0) - \exp(0.0)]^{1/2} = 0.0$

$J(t, t') = q_1 + C_0(t, t') + C_d(t, t', t_0)$

$J(t, t') = 0.1664 + 0.2443 + 0.0 = 0.4107$

Creep strain $= J(t, t')\sigma = 0.4107 \times 1600 = 658 \times 10^{-06}$

Shrinkage strain $= \epsilon_{sh}(t, t_0) = \epsilon_{sh\infty}k_hS(t)$ (Eq. 1.8)

$k_h = -0.2$ $(h = 1)$ (Eq. 1.10)

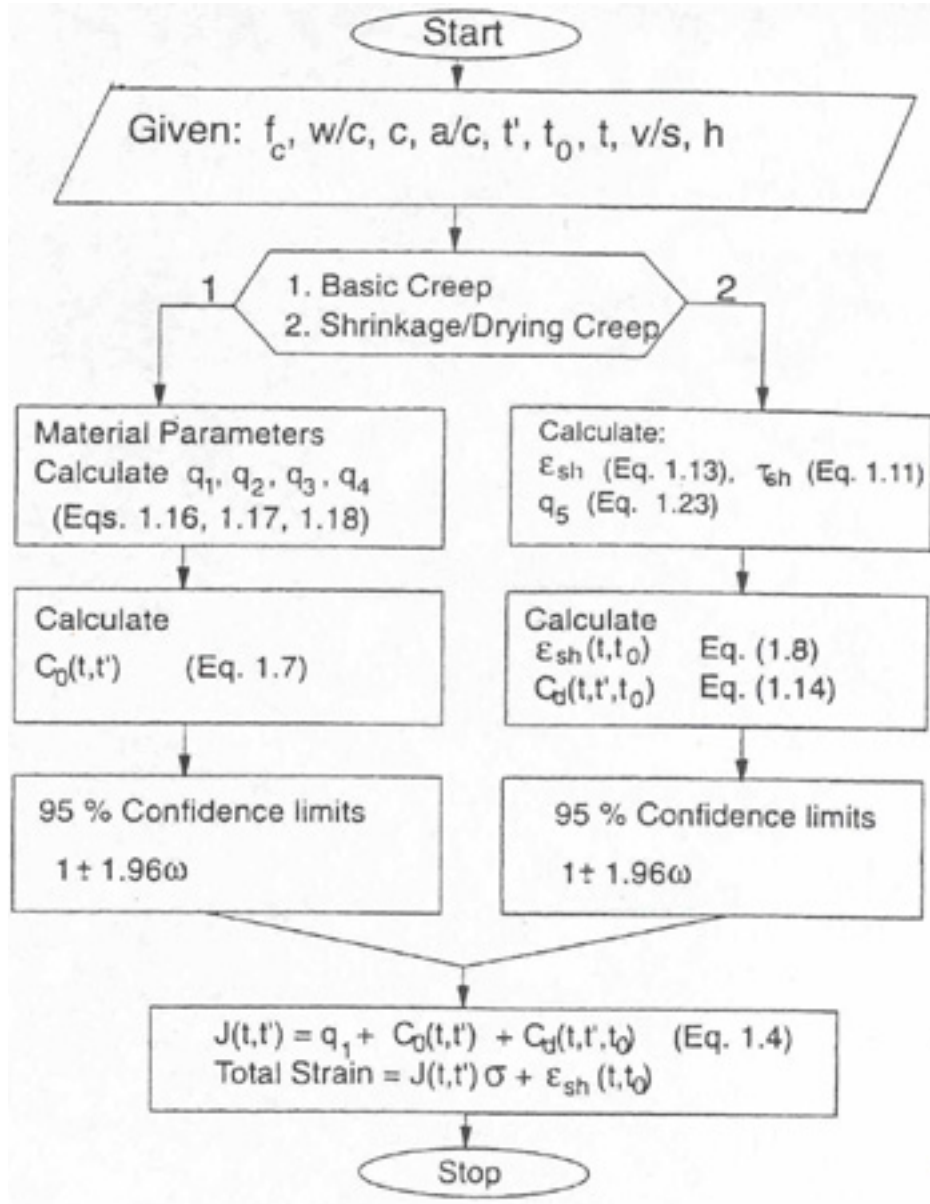Shrinkage strain $= \epsilon_{sh}(t, t_0) = 483.1749 \times -0.2 \times 0.8907 = -86.073 \times 10^{-06}$
    (swelling)

Figure 1.2: Flow chart showing the calculation procedure for Model B3

1.5 Parameter Uncertainties and Statistical Range of Predicted Creep and Shrinkage Values

The parameters of any creep model must be considered as statistical variables. The preceding formulae predicting the creep and shrinkage parameters from the concrete composition and strength give the mean value of $J(t, t')$ and ϵ_{sh}. To take into account the statistical uncertainties, the parameters $q_1, q_2, q_3, q_4, q_5, \epsilon_{sh\infty}$ ought to be replaced by the values

$$\psi_1 q_1, \ \psi_1 q_2, \ \psi_1 q_3, \ \psi_1 q_4, \ \psi_1 q_5, \ \psi_2 \epsilon_{sh\infty} \tag{1.24}$$

in which ψ_1 and ψ_2 are uncertainty factors for creep and shrinkage, which may be assumed to follow roughly the normal (Gaussian) distribution with mean value 1. According to the statistical analysis of the data in the RILEM data bank, the following coefficients of variation of these uncertainty factors should be considered in design[C17]:

$$\begin{aligned} \omega(\psi_1) &= 23\% &\quad \text{for creep, with or without drying} \tag{1.25} \\ \omega(\psi_2) &= 34\% &\quad \text{for shrinkage} \end{aligned}$$

This means that, if the statistical distribution is approximated as Gaussian (normal), the 95% confidence limits for ψ_1 are $1 \pm 1.96 \times 0.23 = 1 \pm 0.45$, and for ψ_2 are $1 \pm 1.96 \times 0.34 = 1 \pm 0.67$.

Some other input parameters of the model are also statistical variables. At least, one should consider in design the statistical variations of environmental humidity h and of strength $\bar{f}_c$. This can be done by replacing them with $\psi_3 h$ and $\psi_4 \bar{f}_c$ where ψ_3 and ψ_4 are uncertainty factors having a normal distribution with mean 1. In the absence of other information and sophisticated statistical analysis, the following coefficients of variation may be considered for these uncertainty factorsß8:

$$\begin{aligned} \omega(\psi_3) &\approx 20\% &\quad \text{for } h \text{ replaced by } \psi_3 h \tag{1.26} \\ \omega(\psi_4) &\approx 15\% &\quad \text{for } \bar{f}_c \text{ replaced by } \psi_4 \bar{f}_c \end{aligned}$$

Factor ψ_3 is statistically independent of ψ_1, ψ_2, and ψ_4. As an approximation, all the factors may be assumed mutually statistically independent[C18,C19].

If the structure is exposed to a climate that is permanently hot or has prolonged high temperature extremes, it is advisable to take into account the temperature effect according to the Appendix to Chapter 1. If this is not done, it is recommended to increase the aforementioned coefficients of variation ω by 10% of ω[16].

1.6 Improved Estimation: Updating Based on Short-Time Tests

A method to improve the prediction based on short-time testsß2 will now be described[C20]. Its use is mandatory for highly creep sensitive structures

characterized as level 5 in Section 1.2.1. It is advisable for level 4, and is useful for level 3. It is not needed for levels 1 and 2.

Updating Creep Predictions
The procedure will be explained by considering as an example, the data for basic creep by L'Hermite et al.ß9, for which the present formulae for the effect of composition and strength do not give a good prediction, as is apparent from Fig. 1.3 (for information on these data see Ref. 3 and 4). We now pretend we know only the first 5 data points for the first 28 days of creep duration, which are shown by the solid circles. We consider that the compliance function is updated by only two update parameters p_1 and p_2, introduced as follows:
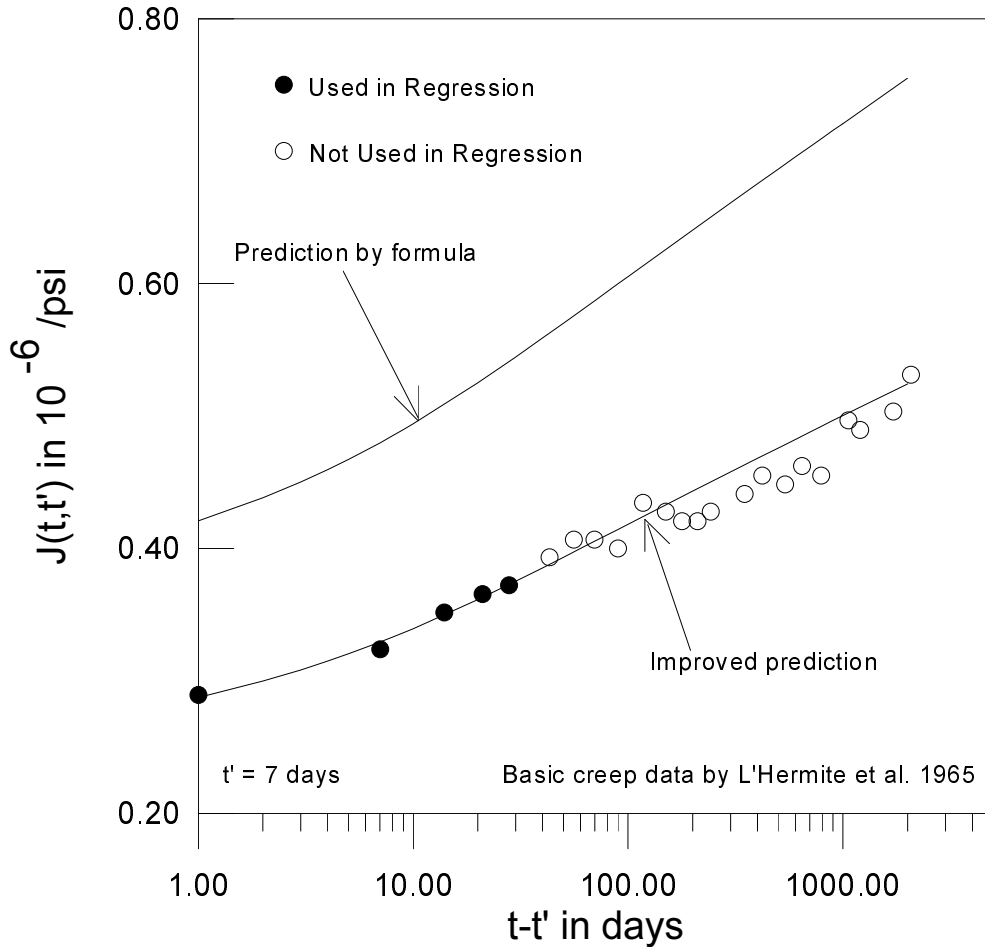

Figure 1.3: Example of improving the prediction of creep by the use of short-time test data

$$J(t, t') = p_1 + p_2 F(t, t') \qquad (1.27)$$

in which

$$F(t, t') = C_0(t, t') + C_d(t, t', t_0) \qquad (1.28)$$

Function $F(t, t')$ is evaluated according to the model, using the formulae for the effect of composition parameters and strength (Eq. 1.16–1.23). If the

15

data agreed with the form of Model B3 exactly, the plot of $J(t,t')$ versus $F(t,t')$ would have to be a single straight line for all t, t' and t_0. The vertical deviations of the data points from this straight line represent errors that may be regarded as random and are to be minimized by least-square regression[C21]. So we consider the plot of the known (measured) short-time values $Y = J(t,t')$ (up to 28 days of creep duration) versus the corresponding values of $X = F(t,t')$, calculated from Model B3, and pass through these points the regression line $Y = AX + B$. The slope A and the Y-intercept B of this line give the values of p_1 and p_2 that are optimum in the sense of the least-square method; $A = p_2$ and $B = p_1$. According to the well-known normal equations of least-square linear regression,

$$p_2 = \frac{n \sum (F_i J_i) - (\sum F_i)(\sum J_i)}{n \sum (F_i^2) - (\sum F_i)^2}, \quad p_1 = \bar{J} - p_2 \bar{F} \qquad (1.29)$$

where $\bar{J}$ = mean of all the measured J_i values, and $\bar{F}$ = mean of all the corresponding F_i values. Using the values $p_1 = B$ and $p_2 = A$, the updated $J(t,t')$ for the concrete tested may be obtained using Eq. 1.27. This updating is equivalent to replacing the values q_1, q_2, q_3, q_4, q_5 calculated from Eq. 1.16 , 1.17, 1.23 by the values $q_1^* = p_1 q_1$, $q_2^* = p_2 q_2$, $q_3^* = p_2 q_3$, $q_4^* = p_2 q_4$, $q_5^* = p_2 q_5$. For the real structure, the ages at loading other than the t'-value used for the test specimens may be needed and the effective thickness, environmental humidity, etc., may be different. To obtain the values of $J(t,t')$ for the real structure one simply evaluates $J(t,t')$ from Eq. (1.4) and (1.6)–(1.15), using parameters $q_1^*, q_2^*, q_3^*, q_4^*, q_5^*$ instead of q_1, q_2, q_3, q_4, q_5 in Eq. 1.4, 1.6–1.15.

As seen in Fig. 1.3, the improvement of long-time prediction achieved by short-time measurements is in this example very significant. The well-known formulae of linear regressionß10 also yield the coefficients of variation of p_1 and p_2, which in turn provide the coefficient of variation of $J(t,t')$ for any given t and t'. (However these formulae might not suffice since the uncertainty of long-time predictions obtained by updating from the short-time data should properly be handled by the Bayesian statistical approachß11,12.)

Updating Shrinkage Predictions

The shrinkage predictions cannot be successfully updated solely on the basis of short-time shrinkage tests alone because of a certain special problem with the shrinkage tests[C22]. This problem can be circumvented if the shrinkage specimens are weighed to determine their relative water loss w (as a percentage of the weight of the concrete), and if also the final relative water loss is estimated by heating the specimens at the end of the shrinkage test in an oven to about 105°C. The water loss should preferably be measured directly on the shrinkage specimens. Anyway, if the water loss is measured on companion specimens, they must be identical and have the same environmental exposure all the time. The following procedure, developed in Ref. 2, is recommended (for a justification, see Sec. 2.3.2–2.3.3 of Chapter 2):

1) Calculate

$$\Delta w_\infty(h) \approx 0.75 \left[1 - \left(\frac{h}{0.98} \right)^3 \right] \Delta w_\infty(0) \quad \text{(for } 0.25 \le h \le 0.96\text{)}$$

(1.30)

where $\Delta w_\infty(h)$ is the estimate of the final relative water loss for drying at given environmental relative humidity h (and room temperature), and $\Delta w_\infty(0)$ is the final water loss that would occur at environmental relative humidity 0, which is taken the same as the average final water loss measured upon heating the specimens to about 105°C.

2) Calculate the auxiliary values

$$\psi_j = \left[\tanh^{-1} \left(\frac{\Delta w_j}{\Delta w_\infty(h)} \right) \right]^2 \quad (j = 1, 2, \ldots m)$$

(1.31)

where Δw_j are the measured values of relative water loss at times t_j $(j = 1, 2, \ldots m)$, which should be spaced approximately uniformly in the scale of $\log(t - t_0)$.

3) Instead of Eq. (1.11), obtain the improved estimate, $\bar{\tau}_{sh}$, of shrinkage half-time from the equation:

$$\bar{\tau}_{sh} = 1.25\tau_w, \qquad \tau_w = \frac{\sum_j (t_j - t_0)\psi_j}{\sum_j \psi_j^2}$$

(1.32)

4) Denote $\epsilon'_{sh_i} = \epsilon'_{sh}(t_i, t_0) =$ measured short-time values of shrinkage at times t_i $(i = 1, 2, \ldots n)$, which should be spaced at approximately constant intervals in the scale of $\log(t - t_0)$ and should preferably coincide with times t_j of water loss measurements. Also denote $\bar{\epsilon}_{sh} = \bar{\epsilon}_{sh}(t, t_0) =$ shrinkage values calculated from Model B3 using $\bar{\tau}_{sh}$ instead of Eq. (1.11). Calculate the values $\bar{\epsilon}_{sh_i} = \bar{\epsilon}_{sh}(t_i, t_0)$ predicted for the times t_i from Model B3 on the basis of $\bar{\tau}_{sh}$ instead of Eq. (1.11). Then calculate the scaling parameter:

$$p_6 = \frac{\sum_i \epsilon'_{sh_i} \bar{\epsilon}_{sh_i}}{\sum_i \bar{\epsilon}_{sh_i}^2}$$

(1.33)

5) The updated values of shrinkage prediction for any time t then are

$$\epsilon^*_{sh}(t, t_0) = p_6 \, \bar{\epsilon}_{sh}(t, t_0)$$

(1.34)

The last equation is equivalent to Eq. (1.8) with (1.9) for the shrinkage of the test specimen if $k_h \epsilon_{sh\infty}$ is replaced by $\epsilon^*_{sh\infty} = p_6 \epsilon_{sh\infty}$ and τ_{sh} is replaced by $\bar{\tau}_{sh}$. To obtain the updated values of $\epsilon_{sh}(t, t_0)$ for the real structure for which t_0, D and h may be different, Eq. (1.19)–(1.20) for $\epsilon_{s\infty}$ and k_t are disregarded. Using the updated value $\bar{\tau}_{sh}$ (instead of the original predicted value τ_{sh}) for the short-time test specimen, Eq. (1.11) is solved for k_t. This yields the updated value, k_t^*, replacing k_t, i.e., $k_t^* = \bar{\tau}_{sh}(k_s D)^{-2}$. Next Eq.

17

(1.13) is used with the updated value $\epsilon^*_{sh\infty}$ (instead of the original value $\epsilon_{sh\infty}$) for the test specimen to solve for the updated value $\epsilon^*_{s\infty}$ that should replace $\epsilon_{s\infty}$, i.e., $\epsilon_{s\infty} = \epsilon^*_{sh\infty}E(t_0 + \bar{\tau}_{sh})/E(607)$. With the updated values, k^*_t and $\epsilon^*_{s\infty}$, and the values of t_0, D, and h for the structure, Eq. (1.8)–(1.13) are used to obtain the updated values of $\epsilon_{sh}(t, t_0)$ for the structure.

The updated $\bar{\tau}_{sh}$ should also be used in the calculation of the drying creep term from Eq. (1.14), which modifies the function $F(t, t', t_0)$ in Eq. (1.28). This improves the previously indicated procedure.

Example of Shrinkage Updating

To illustrate the shrinkage updating procedure, consider the recent shrinkage and water-loss data obtained by Grangerß14 (Fig. 1.4). They measured shrinkage on cylinders with a 16 cm diameter and 100 cm length over a gauge length of 50 cm. The relative weight loss was measured on cylinders with a 16 cm diameter and 15 cm length. The tests were carried out in an environment of 50% relative humidity. The ends of both the shrinkage and the weight-loss specimens were sealed to ensure radial drying. The concrete (Civaux BHP) had a cylindrical compressive strength of 64.3 MPa. The composition of concrete (quantities in kg/m^3) was cement (266), water (161), silica fume (40.3), fine aggregate (782), coarse aggregate (1133), filler (57), and additives (9.98).

We now pretend that we know only the first nine points of data (up to drying duration of 64 days) which are shown as the solid black points in Fig. 1.4. To estimate the final relative water loss, $\Delta w_\infty(0)$, at $h \approx 0$, we assume that the water used up in the hydration reaction is about 20 %, by weight, of the cementitious materials. $\Delta w_\infty(50)$ is calculated using Eq. (1.30). Using this value of $\Delta w_\infty(50)$ and the first nine points of the weight-loss data, we determine $\bar{\tau}_{sh} = 1.25\tau_w$ from Eq. (1.31)–(1.32). This value of $\bar{\tau}_{sh}$ and the drying shrinkage data up to 57 days duration are used in Eq. (1.33)–(1.34) to determine the updated values of shrinkage prediction. Curves, a and b in Fig. 1.4, showing the prediction by formula and the updated prediction, confirm that a significant improvement is achieved.

Fig. 1.4 also shows curve c obtained by trying to match the short-time data solely by vertical scaling of curve a, which is what one would have to do if the water-loss data were unavailable. Although this curve also matches the short-time data quite well, the long-time prediction would in this case become even worse than with curve a before updating. Clearly, updating of τ_{sh} by water-loss data is essential for achieving improved predictions.

Now consider, for example, that the designer needs the value of $\epsilon_{sh}(t, t_0)$ for $D = 25$ cm, $t_0 = 10$ days, and $h = 65\%$. Table 1.2 shows the calculations described in the preceding paragraphs for updating the shrinkage predictions on the basis of the short-time tests and for obtaining, the update parameters for the real structure. Note that the updated material parameters k^*_t and $\epsilon^*_{s\infty}$ are the same for both the specimen and the structure. These update material parameters are used in Eq. (1.8)–(1.13) along with the given values of D, t_0, and h for the real structure to obtain the updated shrinkage values for the real structure.
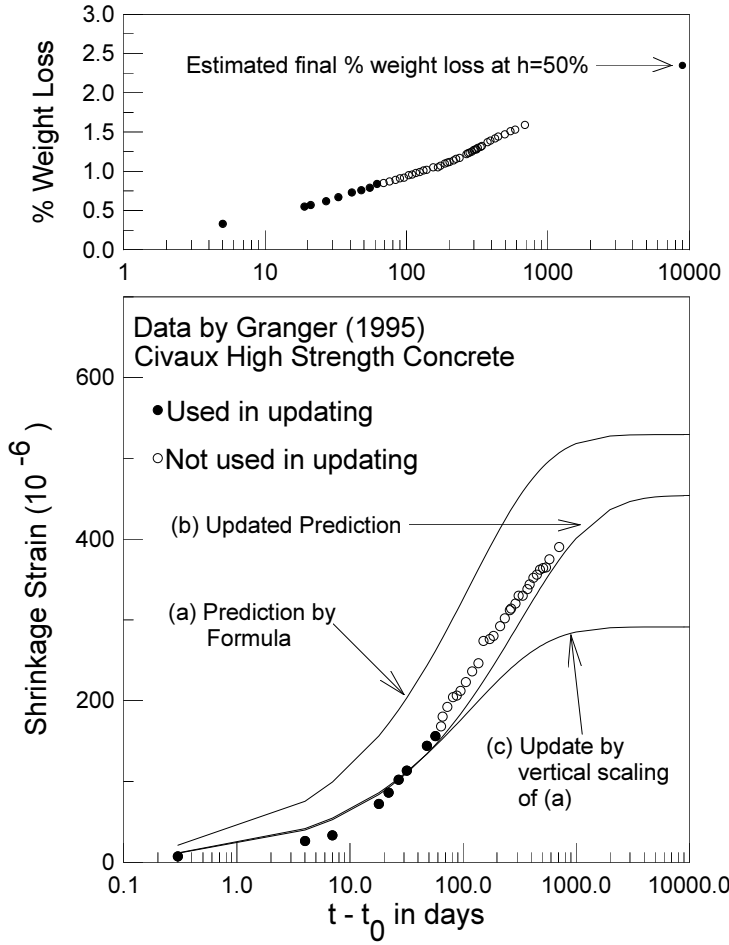
Figure 1.4: Example of updating shrinkage prediction using short-time data and estimated final water-loss

1.7 Appendix to Chapter 1

1.7.1 Approximate Formula for $Q(t, t')$ and Numerical Integration

Instead of Table 1.1, the values of this function can also be obtained from the following approximate formula (derived by Bažant and Prasannan, 1989ß6) which has an error of less than 1% for $n = 0.1$ and $m = 0.5$;

$$Q(t, t') = Q_f(t') \left[1 + \left(\frac{Q_f(t')}{Z(t, t')} \right)^{r(t')} \right]^{-1/r(t')} \tag{1.35}$$

in which

$$r(t') = 1.7(t')^{0.12} + 8, \qquad Z(t, t') = (t')^{-m} \ln[1 + (t - t')^n], \qquad Q_f(t') = [0.086(t')^{2/9} + 1.21(t')^{4/9}]^{-1} \tag{1.36}$$

Table 1.2: Example of Shrinkage Updating Calculations

Parameter	Value
Shrinkage Specimen $D = 2V/S = 8$cm, $t_0 = 28$ days, $h = 50\%$	
τ_{sh} (Eq. 1.11)	195.8
$\epsilon_{sh\infty}$ (Eq. 1.13)	605.2
τ_w (Eq. 1.32)	414.5
$\bar{\tau}_{sh} = 1.25 \times \tau_w$	518.1
$\bar{\epsilon}_{sh\infty}$	601.5
p_6 (Eq. 1.33)	0.86
$\epsilon^*_{sh\infty} = p_6\bar{\epsilon}_{sh\infty}$	517.0
$k^*_t = \bar{\tau}_{sh}(k_s D)^{-2}$	39.5
$\epsilon^*_{s\infty} = \epsilon^*_{sh\infty}E(t_0 + \bar{\tau}_{sh})/E(607)$	516.7
Real Structure, $(D = 25$cm $= 10$in., $t_0 = 10$ days, $h = 65\%)$	
$\tau_{sh} = k^*_t(k_s D)^2$	5221.5
$\epsilon_{sh\infty} = \epsilon^*_{s\infty}E(607)/E(t_0 + \tau_{sh})$	514.9
$\epsilon_{sh}(1010, 10)$ (Eq. 1.8)	153.7

Those who wish to implement numerical integration of Eq. (1.6) on their computer should note that $\lim \dot{C}(t, t') = \infty$ for $t \to t'$. Consequently the integral over the first time interval $\Delta t = t_1 - t'$ should be evaluated analyticallyß6. Use $\Delta t \le 10^{-4}t'$ and $Q(t_1, t') = (t')^{-m}\ln[1 + (\Delta t)^n]$.

1.7.2 Extension to Basic Creep at Constant Elevated Temperature

Eq. (1.6) for the rate of basic creep compliance function is generalized as follows:

$$\dot{C}_0(t, t', T) = R_T\left[\left(q_2\frac{\lambda_0}{t_T} + q_3\right)\frac{n\xi^{n-1}}{\lambda_0(1 + \xi^n)} + \frac{q_4}{t_T}\right] \qquad (1.37)$$

where $\xi = t_T - t'_e$ at current time t and $T = $ absolute temperature. In the foregoing equation, the age at loading and the stress duration are replaced by the following equivalent age and equivalent stress duration:

$$t'_e = \int_0^{t'} \beta_T(t'')dt'', \qquad t_T - t'_e = \int_{t'}^{t} \beta'_T(t')dt' \qquad (1.38)$$

The temperature dependent coefficients are defined by equations[C23]:

$$\beta_T = \exp\left[\frac{U_h}{R}\left(\frac{1}{T_0} - \frac{1}{T}\right)\right] \quad \beta'_T = \exp\left[\frac{U_c}{R}\left(\frac{1}{T_0} - \frac{1}{T}\right)\right] \quad R_T = \exp\left[\frac{U'_c}{R}\left(\frac{1}{T_0} - \frac{1}{T}\right)\right]$$
$$(1.39)$$

$T_0 = $ reference absolute temperature (for all the data fits, $T_0 = 293°$ K); $U_h = $ activation energy of cement hydration; $U_c, U'_c = $ activation energies of creep describing the acceleration of creep rate and magnification of creep due

to temperature increase; and R = gas constant. Integration of Eq. (1.37) yields the basic creep compliance function:

$$C_0(t, t', T) = R_T \left\{ q_2 Q(t_T, t'_e) + q_3 \ln[1 + (t_T - t'_e)^n] + q_4 \ln\left(\frac{t_T}{t'_e}\right) \right\} \quad (1.40)$$

Fitting of the available test data indicates the following parameter values:

$$U_c/R = 110 w^{-0.27} \bar{f}_c^{0.54} \quad \text{(inch-pound system)} \quad = 3418 w^{-0.27} \bar{f}_c^{0.54} \quad \text{(SI)}$$
$$U_h/R = 5000°K, \qquad\qquad\qquad\qquad U'_c = 0.18 U_c$$
$$(1.41)$$

1.7.3 Further Refinements for Highly Sensitive Structures

In the case of structures that are highly sensitive to creep (levels 5 and 4), such as nuclear reactor structures and large span bridges or shells, several other influences on creep and shrinkage should be taken into account in order to reduce the uncertainty of prediction. However extreme caution is necessary for such structures and updating of the model parameters by testing is required.

Creep at Elevated Temperature with Drying

The formulation given in Ref. 4 (part IV, Eq. 9-17) consists of relatively simple explicit expressions. However, it must be warned that explicit formulae can never be very accurate for drying concrete when temperature varies. Only integration of the differential equations of the problem can fulfill such expectations.

Cyclic Environment and Cyclic Loading

These influences can be approximately described by simple explicit expressions given in Ref. 4 (part V, Eq. 1-10).

1.7.4 Uncertainties Due to Time-Variation of Stress and Method of Structural Analysis

The stresses in concrete structures often vary significantly in time. The cause can be the load changes. But even at constant applied loads significant changes of stress can be caused by the stress relaxation due to imposed displacements, by sequential construction with joining of previously disconnected load-carrying members, and by changes of restraints of the structure. Significant stress variation can also be caused by differences in shrinkage and creep of joined structural parts of different age, of parts made of different materials (different concretes or concrete and steel), of parts of different thickness or different hygrothermal conditions, etcß15-18.

In such cases the effect of stress variation is calculated according to the principle of superposition. This causes additional *errors of two kinds*: (1) an error of the principle of superposition per se, and (2) an error in the approximate method of analysis compared to the exact solution according to the principle of superpositionß15. Estimation of these errors is a complex question that needs to be researched more deeply but the following simplified approach is better than ignoring these errors altogether.

Let ω_X be the coefficient of variation of some response such as the deflection or the maximum stress in the structure. Let $\lambda_L = \max(\Delta P/P_{\max},\ \Delta\sigma/\sigma_{\max})$ where $\Delta P = P_{max} - P_{min}$ and $\Delta\sigma = \sigma_{max} - \sigma_{min}$ where $P_{max}, P_{min}, \sigma_{max}, \sigma_{min}$ are rough estimates of the maximum and minimum values of load P and stress σ during the lifetime of the structure. For a constant load, $\lambda_L = 0$. Then one should replace ω_X by $\omega_X + \Delta\omega_X$ where the increase $\Delta\omega_X$ of the coefficient of variation may be taken approximately as follows:

$$\begin{aligned} \Delta\omega_X &= 0.05\lambda_L \qquad \text{for class I methods} \qquad\qquad (1.42)\\ &= 0.07\lambda_L \qquad \text{for class II methods}\\ &= 0.25\lambda_L \qquad \text{for class III methods} \end{aligned}$$

Coefficient λ_L takes into account errors of the first kind and the classes of methods take into account the errors of the second kind. The class I methods are the computer methods of structural creep and shrinkage analysis that solve the problem accurately according to the principle of superposition (using either integral equations or the Maxwell or Kelvin chain approximations, solved in small time steps). The class II methods are the simplified methods of good accuracy, such as the age-adjusted effective modulus method. The class III methods are crude simplified methods such as the effective modulus method, the rate-of-creep (Dischinger) method and the rate-of-flow method.

Approximate knowledge of the coefficient of variation provides a rational basis to the designer for deciding how sophisticated a method should be used. Simple but crude methods for predicting creep and shrinkage of concrete can be used but the important point is that their coefficients of variation should be considered. If the designer regards the coefficient of variation (or the 95% confidence limits) of the deflection or stress obtained for the effective modulus method as acceptable (not uneconomic), he can use that method and need not bother using a more complicated method of structural analysis. The coefficient of variation depends on the type of structure and type of response. For example, the deflection of a small-span nonprestressed reinforced concrete beam is a problem relatively insensitive to creep, and a very simple estimation based on the effective modulus method is adequate, as documented by a small coefficient of variation and small mean values of deflections. On the other hand, the deflection of a large-span prestressed box girder bridge is a creep-sensitive problem, which is manifested by a high coefficient of variation of the deflection or maximum stress. For such problems it pays to use the most sophisticated method.

1.7.5 Free Shrinkage and Thermal Strain as a Constitutive Property

Some sensitive structures are analyzed by layered beam finite element programs or by two and three dimensional finite element programs. In such programs, the material properties used in each finite element must be the constitutive properties, independent of the cross-section dimensions and shape as well as the environmental conditions (which represent the boundary conditions for partial differential equationsß19). At drying, the constitutive properties cannot be measured directly, but they have been identified by fitting with a finite element program the overall deformation measurements on test specimensß20-23). For this kind of analysis, only Eq. (1.3), (1.4) and (1.6) [or (1.11)] are retained, while Eq. (1.8)–(1.15) and (1.37)–(1.41) must be deleted and replaced by the following constitutive relationß20 for the strain that must be added to the basic creep strain (with elastic deformation):

$$\dot{\epsilon}_{s_{ij}} = \epsilon_s^0 \frac{E(t_0)}{E(t)} [\delta_{ij} + s_h(r\sigma_{ij} + r'\sigma^v \delta_{ij})](\dot{h}_l + a_T \dot{T}_l) \qquad (1.43)$$

Subscripts i, j refer to Cartesian coordinates x_i $(i, j = 1, 2, 3)$; superimposed dots denote time rates (i.e., $\partial/\partial t$); δ_{ij} = Kronecker delta; σ_{ij} = stress tensor; σ^v = volumetric (or mean) stress; ϵ_s^0 = final shrinkage (at material points), which has a similar but not exactly the same value as $\epsilon_{sh\infty}$ for the cross-section average; $\dot{h}_l$ and $\dot{T}_l$ = rates of local relative humidity and temperature in the pores of concrete (which must be obtained by solving the diffusion equations); s_h = sign of $(\dot{h}_l + a_T\dot{T}_l)$, which is 1 or -1; and a_T = coefficient relating the stress-induced thermal strain and shrinkage. When Eq. (1.43) is used, the cracking or fracture must also be included in the analysis.

The constitutive relation (1.43) is much simpler than Eq. (1.8)–(1.15) and (1.19)–(1.23) which it replaces. However, at present there are not enough data to predict the values of ϵ_s^0, r, r' and a_T from the composition and strength of the concrete. They must be identified by fitting the given data for drying creep, shrinkage and thermal expansion.

1.7.6 Simplified Approximate Method of Structural Analysis for Creep and Shrinkage

Theoretically exact solutions according to the principle of superposition lead to integral or differential equations. Although computer methods for such equations are accurate and effective, for most practical problems it suffices to use a much simpler approximate method—the age-adjusted effective modulus method, which converts the problem to elastic structural analysis. This method was recommended in ACI 209 and its basic applications were described in Chapters 3-5 of that report. These descriptions remain valid except the table listing the values of the aging coefficient, χ, (Table 5.1.1) because χ depends on the creep model, which is different in this report. A list of values of the aging coefficient χ for the present model for one set of typical values of constitutive parameters q_1, q_2, q_3, q_4 is given in Table 1.3. The

Table 1.3:   Values of the Aging coefficient, χ for a set of typical values of material parameters.

$q_1 = 0.2, q_2 = 0.4, q_3 = 0.02, q_4 = 0.07 \ (\times 10^{-6}/\text{psi})$				
	$t - t'$ (days)			
t'	10	100	1000	10000
1	0.462	0.445	0.490	0.547
10	0.706	0.588	0.593	0.634
100	0.877	0.709	0.625	0.643
1000	0.942	0.887	0.706	0.640

aging coefficient can be easily calculated using the relation:

$$\chi(t, t') = \frac{E(t')}{E(t') - R(t, t')} - \frac{1}{\phi(t, t')} \tag{1.44}$$

where $R(t, t')$ is the relaxation function, and $\phi(t, t')$ is the creep coefficient. For the relaxation function, $R(t, t')$ the following approximation can be usedß24:

$$R(t, t') = \frac{0.992}{J(t, t')} - \frac{0.115}{J_0}\left[\frac{J(t' + \xi, t')}{J(t, t - \xi)} - 1\right]; \quad J_0 = J(\xi + t', \xi + t' - 1) \tag{1.45}$$

where $\xi = (t - t')/2$. For the compliance function considered in Ref. 24, $J_0 = J(t, t - 1)$, as recommended in ACI 209-R92. However the expression for J_0 in Eq. (1.45) was found to give more accurate results for the present compliance function.

For more detailed information on the age-adjusted effective modulus method see Ref. 25 and 26.

1.7.7   Notation

a/c = aggregate-cement ratio, by weight;

c = cement content of concrete in lb/ft^3 (in kg/m^3 for the SI version, 1 lb/ft^3= 16.03 kg/m^3);

$C_0(t, t')$ = compliance function for basic creep only;

$C_d(t, t', t_0)$ = compliance function for additional creep due to drying;

$D = 2v/s$ = effective cross section thickness in inches (in mm for the SI version, 1 inch = 25.4mm);

$\bar{f}_c$ = mean 28-day standard cylinder compression strength in psi (in MPa for the SI version, 1 psi = 6895 Pa) (if only design strength f'_c is known, then $\bar{f}_c = f'_c + 1200$ psi);

$F(t, t')$ = function used in creep updating;

h = relative humidity of the environment (expressed as a decimal number, not as percentage) $0 \le h \le 1$;

H = spatial average of pore relative humidity within the cross section, $0 \le H \le 1$;

$J(t, t')$ = compliance function = strain (creep plus elastic) at time t caused by a unit uniaxial constant stress applied at age t' (always given in 10^{-6}/psi, the SI version of the formulae give $J(t, t')$ in 10^{-6}/MPa, 1 psi = 6895 Pa);

k_t = parameter used in calculation of τ_{sh};

k_h = humidity correction factor for final shrinkage;

p_1, p_2 = parameters used in creep updating;

p_6 = parameter used in shrinkage updating;

q_1, q_2, q_3, q_4, q_5 = empirical material constitutive parameters given by formulae based on concrete strength and composition;

$R(t, t')$ relaxation function;

$S(t)$ = time function for shrinkage;

t = time, representing the age of concrete, in days;

t' = age at loading, in days;

t_0 = age when drying begins, in days (only $t_0 \leq t'$ is considered);

v/s = volume-to-surface ratio in inches;

w/c = water-cement ratio, by weight;

$w = (w/c)c$ = water content of concrete mix in lb/ft^3 (in kg/m^3 for the SI version;

$\chi(t, t')$ aging coefficient;

$\Delta w(h)$ = relative water (weight) loss at relative humidity h;

$\epsilon_{sh}, \epsilon_{sh\infty}$ = shrinkage strain and ultimate (final) shrinkage strain; $\epsilon_{sh\infty} \geq 0$ but ϵ_{sh} is considered negative (except for swelling, for which the sign is positive); always given in 10^{-6};

$\bar{\epsilon}_{sh}, \epsilon'_{sh}$ = shrinkage values given by the formula and measured shrinkage values used in the updating procedure;

$\phi(t, t')$ creep coefficient;

τ_{sh} = shrinkage half-time in days;

$\bar{\tau}_{sh}$ = updated value of τ_{sh};

θ = relative water content;

All symbols marked with an asterisk represent the corresponding parameters updated using short-time tests.

1.7.8 Commentary and Explanations

[C1] A more precise classification of the level of sensitivity of a structure could be made on the basis of the coefficients of variation of responses such as deflection or stress or even better on the basis of sensitivity analysis. But such an approach might be cumbersome for practice and would anyway require further research.

[C2] The numbers 0.85 for w/c ratio and 10 lbs/ft^3 or 45 lbs/ft.^{3} for cement content are of course outside the range of good concretes in today's practice.

[C3] Formulae predicting model parameters from the composition of concrete have not been developed for special concretes containing various admixtures, pozzolans, microsilica, and fibers. However, if the model parameters are not predicted from concrete composition and strength

but are calibrated by experimental data, the model can be applied even outside the range of applicability in section 1.2, for example, to high-strength concretes, fiber-reinforced concretes, and mortars.

[C4] This means that creep may be assumed to be linearly dependent on stress

[C5] When stresses vary in time, the corresponding strain can be approximately calculated from Eq. (1.3) according to the principle of superposition as recommended by RILEM committee guidelinesß1. Simplified design calculations can be done according to the age-adjusted effective modulus methodß25,26, which allows quasi-elastic analysis of the structure.

[C6] Generalization to multiaxial stress may be based also on the principle of superposition. The creep Poisson ratio may be assumed to be constant and equal to the instantaneous Poisson ratio $\nu = 0.18$. (Tensile microcracking can cause the apparent Poisson ratio to be much smaller, but this is properly taken into account by a model for cracking.)

[C7] The instantaneous strain, which is the same as in previous models BP and BP-KXß3,4, may be written as $q_1 = 1/E_0$ where E_0 is called the asymptotic modulus. E_0 should not be regarded as a real elastic modulus but merely as an empirical parameter that can be considered as age-independent. The age-independence of E_0 is demonstrated by the experimental fact (reported in 1976 by Bažant and Osmanß27) that the short-time creep curves for various t', plotted as $J(t, t')$ versus $(t - t')^n$ (with $n \approx 0.1$), appear approximately as straight lines all of which meet for $t - t' = 0$ approximately at the same point, regardless of t' (see Fig. 2.8d,e in Chapter 2). As a rough estimate, $E_0 \approx 1.5E$. The use of E_0 instead of the conventional static modulus E is convenient because concrete exhibits pronounced creep even for very short load durations, even shorter than 10^{-4} s. The usual static elastic modulus E normally obtained in laboratory tests and used in structural analysis corresponds to

$$E(t') = 1/J(t' + \Delta, t') \tag{1.46}$$

in which the stress duration $\Delta = 0.01$ day gives values approximately agreeing with ACI formula, $E(t) = 57,000\sqrt{\bar{f}_c(t)}$, with E and $\bar{f}_c$ in psi (or $E(t) = 4734\sqrt{\bar{f}_c(t)}$ with E and $\bar{f}_c$ in MPa). For short-time loading $(t - t' \ll t')$, Eq. (1.46) and Eq. (1.4) along with Eq. (1.7) stated later give the age-dependence:

$$E(t') = \frac{1}{A_0 + A_1/\sqrt{t'}} \tag{1.47}$$

where $A_0 = q_1 + q_3 \ln(1 + \Delta^n)$, $A_1 = q_2 \ln(1 + \Delta^n)$, $A_0, A_1 = $ constants and Δ is in days. q_1, q_2, q_3 are material constitutive parameters given by formulae based on the concrete strength and composition. This age-dependence agrees with the test data on $E(t')$ even better than the current ACI formula, $E(t) = E(28)[t/(\alpha + \beta t)]^{0.5}$, in which α, β are constants (see Fig. 2.10), but the difference is unimportant. For $\Delta = 10^{-7}$ day Eq. (1.47) gives also realistic values of the dynamic modulus of concrete and its age dependence. The graphical meaning

of the values of $q_1 = 1/E_0$ and $1/E$ is explained in Fig. 1.1. Note that for structural analysis it is not important which value of Δ corresponds to $E(t')$ in Eq. (1.5), and not even whether some other definition of E is used in Eq. (1.5). One could use the ACI formula, $E(t) = 57000\sqrt{\bar{f}_c(t)}$, with E and $\bar{f}_c$ in psi (or $E(t) = 4734\sqrt{\bar{f}_c(t)}$ with E and $\bar{f}_c$ in MPa) or Eq. (1.46) for any value of $\Delta \leq 0.1$ day. For the results of structural analysis of creep and shrinkage (for $t - t' \geq 1$ day), the only important aspect is that $E(t)$ and $\phi(t,t')$ together must give the correct total compliance $J(t,t') = [1+\phi(t,t')]/E(t')$, as used by Model B3.

^{C8} Note that if a prediction model would specify $\phi(t,t')$ instead of $J(t,t')$, there would be a danger of combining $\phi(t,t')$ with some incompatible value of $E(t)$ which would result in wrong $J(t,t')$ values. There are many combinations of $\phi(t,t')$ and $E(t)$ that give the same $J(t,t')$. What matters for structural creep calculations is only the values of $J(t,t')$, and not the values of ϕ and E that yield $J(t,t')$. Care in this regard must also be taken when updating the model parameters from some test data for which only the values of $\phi(t,t')$ were reported. $J(t,t')$ cannot be calculated from such data using a definition of E. For example, $E = 57000\sqrt{\bar{f}_c}$, may not give values compatible with these ϕ-values and may give a $J(t,t')$ disagreeing with Eq. (1.5). Conversions of such data from ϕ to J-values must be based on short-time strains or E-values measured on the creep specimens themselves, or else such data cannot be used.

^{C9} In normal concretes this decrease is small (to about 96%-98%).

^{C10} This means that the normal strain $J(t,t')\sigma$, representing the sum of the elastic and creep strains, is measured by subtracting the deformations of a loaded specimen and a load-free companion. For shear creep this is not necessary because shrinkage is strictly a volume change.

^{C11} Autogenous shrinkage terminates if the relative humidity in the pores drops below approximately 85%. Further shrinkage (or expansion) may be caused by various chemical reactions, for example carbonation. But in good concretes, carbonation occurs only in a surface layer a few millimeters thick and can be neglected for normal structures. For concrete submerged in water ($h =100\%$), there is positive ϵ_{sh}, that is, swelling, which is approximately predicted by the present model upon substituting $h =100\%$.

^{C12} Note that the computer solutions of structural creep problems in small time steps require only the rate of compliance $\dot{J}(t,t')$, not the total value $J(t,t')$:

^{C13} $Q(t,t')$ is a binomial integral, which cannot be expressed analytically.

^{C14} Note that ϵ_{sh} is relatively insensitive to the precise definition of E and either formula for $E(t)$ yields about the same result[13]. For simplified analysis one can assume $\epsilon_{sh\infty} \approx \epsilon_{s\infty}$. The typical values of $\epsilon_{sh\infty}$ according to Eq. (1.13) range from 300×10^{-6} to 1100×10^{-6}. The value of elastic modulus $E(t)$ can be expressed either from Eq. (1.46)

of the present model or approximately from the equation $E(t) = E(28)[t/(4+0.85t)]^{1/2}$. This equation (which is used in ACI 209), has been adopted for the present fitting of data; it does not fit the data on the age-dependence of E as well as Eq. (1.47) but the difference is unimportant. Because $\tau_{sh} \propto D^2$, Eq. (1.13) also approximately describes the effect of D on $\epsilon_{sh\infty}$, which is caused by the fact that thicker specimens reach a higher degree of hydration because their core remains wet for a longer time, and the fact that they undergo more microcracking, which reduces shrinkage. The present model does not describe separately the autogenous shrinkage which occurs in sealed specimens (or mass concrete). Such shrinkage is caused by volume changes during the chemical reactions of hydration and is independent of the size of the specimen. This shrinkage is usually much smaller than the drying shrinkage. In exposed specimens there is some autogenous shrinkage too, but is still smaller because: (1) most of it occurs before stripping the mold, and (2) after stripping the mold it occurs only in the core and only until the drying front reaches the core. This part of autogenous shrinkage is included in the present model because the model was fitted to the total shrinkage data for drying specimens.

[C15] Predicting the creep and shrinkage properties of concrete from the composition of concrete mix and the strength of concrete is an extremely difficult problem for which no good theory has yet been developed. The present formulae which are partly empirical and partly reflect trends theoretically deduced from the understanding of physical mechanisms, were calibrated by statistical analysis of the data in a computerized data bank involving about 15,000 data points and about 100 test series.

[C16] Alternatively, from the approximate formulae, $Z(t,t') = (t')^m \ln[1 + (t-t')^n] = 0.1775$, $Q_f(t') = [0.086(t')^{2/9} + 1.21(t')^{4/9}]^{-1} = 0.1818$, and $Q(t,t') = Q_f(t')\{1 + [Q_f(t')/Z(t,t')]^{r(t')}\}^{-1/r(t')} = 0.1818 \times \{1 + [0.1818/0.1785]^{10.5358}\}^{-0.0949} = 0.1681$.

[C17] The present report does not rule out using the previous model in Chapter 2 of ACI 209. However, if this is done, one must consider the predicted creep and shrinkage to have coefficients of variations of 58%.

[C18] The coefficients of variation in Eq. (1.26-1.27) can result in similar or very different (much smaller or much larger) coefficients of variation of structural response such as the predicted maximum deflection or the maximum stress in the structure. If the safety against collapse is threatened, as in long-time creep buckling of shell roofs, structures should not be designed for the mean effects of creep and shrinkage. Rather they should be designed for the response (deflection, stress, strain) values representing the 95% confidence limits. This means that, if 20 identical structures were built and subjected to the same loading and environment, only one of them would be likely to suffer intolerable deflections or cracking damage, whereas the design for mean response means that 10 of them would be likely to suffer such a fate. One may assume the response values to have a normal (Gaussian)

distribution, and then the 95% confidence limits may be estimated as (mean of X) $\times (1 \pm 1.96 \omega_X)$; ω_X can be calculated by generating in a proper wayß26 about 10 random samples of material parameters and then running for each sample a deterministic structural analysisß8.

[C19] The large uncertainty in the prediction of creep and shrinkage of concrete, reflected in the values of the coefficients of variation in Eq. (1.26), is caused mainly by the effect of the composition and strength of concrete. This effect is very complicated and is handled at present empirically because its mathematical theory is not yet available. At present, the only way to reduce the uncertainty is to conduct short-time tests and use their results to update the values of the material parameters in the model. This approach is particularly effective for creep but is more difficult for shrinkageß13.

[C20] The largest source of uncertainty of creep and shrinkage prediction model is the dependence of the model parameters on the composition and strength of concrete. This uncertainty can be greatly reduced by carrying out on the given concrete short-time creep and shrinkage measurements (of duration less than 1 to 3 months) and adjusting the values of the model parameters accordingly. This is particularly important for special concretes such as high-strength concretes or fiber-reinforced concretes. Various types of admixtures, superplasticizers and pozzolanic ingredients used in these concretes have been found to have a significant effectß28,29. Empirical formulae for the effects of all these ingredients on the model parameters would be very difficult to formulate because of the great variety of additives and their combinations. For the planning of short-time creep measurements, note that the prediction improvement based on short-time data is more successful if the creep measurements begin at very short times after the loading (and likewise for shrinkage, if the measurements begin immediately after the stripping of the mold). Also, the measurements should be taken at approximately constant intervals in log-time, e.g. at 30, 100, 300, 1000, 3000... seconds. The reason is that the creep curves rise smoothly through the entire range from 0.0001 s to 30 years. In our example, the first reading was taken as late as 1 day after loading, as is often done, and therefore as many as 28 days of creep data were needed for prediction improvement. In a similar example using a different data set, it was shownß12 that if the first reading is taken as soon as possible after loading (within 1 minute) and about six readings are taken during the first two days of load duration (uniformly spaced in log-time), a similar improvement can be achieved using those readings only. Thus the required duration of the short-time test could be reduced if the readings begin immediately after loading. Anyhow, for reliable prediction of creep values for over five years of creep duration, it is recommended to carry out short-time tests of at least 28 day duration (with the first reading immediately after the loading and further readings equally spaced on the logarithmic scale of creep duration).

^{C21} An important advantage of the present model is that all the free parameters for creep with elastic deformation, that is, q_1, q_2, q_3, q_4, q_5, are contained in the formulae linearly. Therefore, linear regression based on the least-square method, which minimizes the value of $\bar{\omega}^2_{all}$, can be used to identify these parameters from test data. The same is true of parameter $\epsilon_{sh\infty}$ for shrinkage. Thus the only nonlinear parameter of the entire Model B3 is the shrinkage half-time τ_{sh}.

^{C22} The reason is that the shrinkage half-time τ_{sh} is involved nonlinearly and in such a manner [seen from Fig. 2.11 (a,b)] that very different values of τ_{sh} can yield almost equally good fits given short-time data (except if the data reach well beyond the time at which the slope of ϵ_{sh} versus $\log(t - t_0)$ begins to level off).

^{C23} These equations represent Arrhenius equations based on the activation energy theory

Chapter 2

Justification and Refinements of Model B3

2.1 Introduction

Realistic prediction of concrete creep and shrinkage is of crucial importance for durability and long-time serviceability of concrete structures, and in some cases also for long-time stability and safety against collapse. Mispredictions of this phenomenon, which contribute to excessive deflections and cracking, have been one of the reasons for problems with longevity of the civil engineering infrastructure in all countries. The errors in the prediction of concrete creep and shrinkage have generally been larger than the errors caused by simplifications in the methods of structural analysis. It is now clear that, for creep sensitive structures, it makes little sense to use finite element analysis or other sophisticated computational approaches if a realistic model for creep and shrinkage is not introduced in the input. If a simplistic and grossly inaccurate prediction model for creep and shrinkage is used for a creep sensitive structure, one can hardly justify anything more than simple hand calculations of stresses and deformations in structures. In such a case, it makes no sense for the analyst to spend weeks on the computer analysis of the structure while spending half an hour to determine creep and shrinkage properties to use as the input. The design will be better if more time is devoted to the latter than the former.

Realistic prediction of creep and shrinkage of concrete is a formidably difficult problem because the phenomenon is a result of several interacting physical mechanisms and is influenced by many variable factors. In view of this fact, it is not surprising that improvements have been only gradual and slow. No sudden breakthrough has occurred. However, the accumulated advancement of knowledge since the early systematic researches in the 1930's, and especially during the last two decades, has been enormous. It is now possible to formulate a much better prediction model than two decades ago.

Four major advances have made a significant prediction improvement possible:

1. Improved theoretical understanding, for example, of mathematical mod-

eling of the solidification process of cement, diffusion processes, thermally activated processes, cracking damage, residual stresses, and non-uniformity of stress and pore-humidity profiles.

2. Gradual accumulation of test data and formulation of an extensive computerized data bank, which started with the Northwestern University data bank in the 1970's[3] having over 10,000 data points. Subsequently, in collaboration with ACI and CEB, this developed into the RILEM Data Bank, compiled by Subcommittee 5 of RILEM Committee TC-107 (chaired by H. Müller). (This data bank now comprises about 600 measured time curves from about 100 test series from various laboratories around the world, with about 15,000 data points.)

3. Progress in statistical evaluation of test data, optimization of the creep and shrinkage prediction model and optimization that minimizes the sum of the squares of errors. This task has been facilitated by the computerized form of the aforementioned RILEM data bank.

4. Numerical studies of the response of test specimens and structures (especially by finite elements) and their comparisons with observed behavior, which has shed light on various assumptions on the material model used in the input.

Much of the complexity and error of the prediction model is caused by the fact that the design offices still analyze most structures according to beam theory, which requires the average material characteristics for the cross section of the beam as a whole. Because the material creep and shrinkage properties inevitably become non-uniform throughout the cross section (due to diffusion phenomena, residual stresses, cracking, damage localization and fracture), the model for the average material properties in the cross section is not a material constitutive model. It depends on many more influencing factors than the constitutive model, such as the shape of the cross section, environmental history, ratios of the bending moment, normal force and shear force.

For this reason, a really good model for the prediction of the average shrinkage properties and average creep at drying in the cross section under general loading and environmental conditions will never be possible. One must accept significant errors, increased complexity, and a greater number of empirical parameters if one insists on characterizing the behavior of the cross section as a whole by its average properties. In the future, the design approach should move away from characterizing the cross section creep and shrinkage properties of the cross section as a whole, and toward an approach in which the cross sections are subdivided into individual small elements. However, for the time being, an integral prediction model for the cross section as a whole is needed. In the special case of constant temperature and constant moisture content, the average characterization of creep in the cross section is identical to a constitutive model for a material point. In that case, the model becomes far simpler and more accurate.

The present model, which for brevity, is labeled Model B3 and is based on reportß2, is the third major refinement in a series of models developed at Northwestern University, including the BP modelß3 and BP-KX modelß4. Model B3 is simpler, better supported theoretically and as accurate as these previous models. Research progress will not stop, and no doubt further improved versions will become possible in the future. Compared to the latest BP-KX model, the improvement in Model B3 consists in simplification of the formulae achieved by sensitivity analysis, incorporation of a theoretically derived rather than empirical expression for the drying creep, and calibration of the model by an enlarged data set including the data published in the last few years.

Model B3 conforms to the guidelines that have recently been formulated by RILEM Committee TC-107, as a refinement and extension of the conclusions of a preceding RILEM Committee TC-69ß1. These guidelines summarize the basic properties of creep and shrinkage that have been well established by theoretical and experimental researches and represent the consensus of the committee. The existing prediction models of major engineering societies violate many of these guidelines. The present model must nevertheless be regarded as only an example of a model satisfying these guidelines because formulation of a model based on the guidelines is not unique and conceivably partly different models satisfying these guidelines could be formulated, too.

The purpose of this Chapter 2 is to provide justification as well as some refinements of Model B3. All the notations from Chapter 1 are retained.*

2.2   Unbiased Statistical Evaluation Based on Computerized Data Bank

Development of a data bank comprised of practically all the relevant test results on creep and shrinkage of concrete obtained in various countries and laboratories up to the present time facilitates evaluation and calibration of creep and shrinkage prediction models. No longer tediousness limits such evaluation to a few subjectively selected test data. It is important to use the complete set of available test data, because subjective selections of some data for verification of a creep model have been shown to be capable of greatly distorting the conclusions.

The statistical evaluation and optimization of Model B3 has been carried out in the same manner as for the preceding models BP and BP-KX (See Ref. 3–Part 6; Ref. 4 and Ref. 13). Optimum values of the model parameters that minimize the sum of squared deviations from the data in the data bank have been determined. The deviations of the model from the test data (errors) have been characterized by their coefficient of variation $\bar{\omega}$ which is defined

---

*The same model as described here has been proposed to the RILEM committee TC-107. A favorable consensus has been achieved in that committee and the model will now be submitted for public discussion as a possible RILEM recommendation.

for the data set number j as

$$\bar{\omega}_j = \frac{s_j}{\bar{J}_j} = \frac{1}{\bar{J}_j}\sqrt{\frac{1}{n-1}\sum_{i=1}^{n}(w_{ij}\Delta_{ij})^2}, \tag{2.1}$$

in which

$$\bar{J}_j = \frac{1}{n}\sum_{i=1}^{n}w_{ij}J_{ij}, \qquad w_{ij} = \frac{n}{n_d n_1} \tag{2.2}$$

Here J_{ij} are the measured values (labeled by subscript i) of the compliance function in the data set number j; n is the number of data points in the data set number j; Δ_{ij} is the deviation of the value given by the model from the measured value; s_j is the standard deviation of Δ_{ij} values for set j; w_{ij} are the weights assigned to the data points; n_d is the number of decades on the logarithmic scale spanned by measured data in data set number j; and n_1 is the number of data points in one decade.

The weight assigned to a data point in a decade on the logarithmic scale is taken as inversely proportional to the number of data points, n_1, in that decade and the weights are normalized such that $\sum_i w_{ij} = n$. The use of $n-1$ in (2.1) is required for an unbiased estimate of s_j. The overall coefficient of variation of the deviations of the model from the measured values for all the data sets in the data bank has been defined as

$$\bar{\omega}_{all} = \sqrt{\frac{1}{N}\sum_{j=1}^{N}\bar{\omega}_j^2} \tag{2.3}$$

in which N is the number of data sets in the bank (in Table 2.1, the $\bar{\omega}_j$ values are those on line 1 to 17, in Table 2.2 those on lines 1 to 21, etc). Similar expressions, with J replaced by shrinkage strain ϵ_{sh}, have been used for shrinkage. Eq. (2.3) represents the standard deviation of the population of relative errors $\Delta_{ij}/\bar{J}_j$ of all the test series put together, with the same weight on each test series rather than on each reading. One might be tempted to use the alternative formula $\bar{\omega}_{all} = [\sum_j s_j^2/N]^{1/2}/\tilde{J}$ with $\tilde{J} = \sum_j \bar{J}_j/N$, which is based on the population of actual rather than relative errors, or the formula $[\sum_i\sum_j(w_{ij}\Delta_{ij})^2/Nn - 1]^{1/2}/\hat{J}$ with $\hat{J} = \sum_i\sum_j J_{ij}/Nn$, which is based on the population of Δ_{ij} of all the test series put together. But the former would give more weight to weaker concretes (because they creep more) and the latter to those test series for which more readings were taken (the number of readings is partly a subjective choice).

The statistics of the errors of Model B3 in comparison to the test data sets in the RILEM data bank are given in Tables 2.1–2.3 for basic creep, shrinkage and creep at drying. For comparison, the statistics of errors of the current ACI modelß5, developed in the mid-1960's by Branson et al., and the latest CEB modelß30 are also shown (for a comparison to another recently proposed modelß31 see the discussion of Ref. 31). Table 2.4 presents the statistics of the extension of the model to basic creep at constant elevated temperatures. Figs. 2.1–2.4 show some typical comparisons with selected important test dataß33-44 from the data bank.

Table 2.1: Coefficients of variation of errors (expressed as percentage) of basic creep predictions for various models.

Model	B3	ACI	CEB
Test data	$\bar{\omega}$	$\bar{\omega}$	$\bar{\omega}$
1. Keeton	19.0	37.5	42.8
2. Kommendant et al	15.3	31.8	8.1
3. L'Hermite et al.	49.4	133.4	66.2
4. Rostasy et al.	15.2	47.6	5.0
5. Troxell et al.	4.6	13.9	6.2
6. York et al.	5.6	37.7	12.8
7. McDonald	6.9	48.4	22.2
8. Maity and Meyers	33.8	30.0	15.7
9. Mossiossian and Gamble	18.6	51.5	47.3
10. Hansen and Harboe et al. (Ross Dam)	14.1	51.2	31.1
11. Browne et al. (Wylfa vessel)	44.7	47.3	53.3
12. Hansen and Harboe et al. (Shasta Dam)	22.7	107.8	43.1
13. Brooks and Wainwright	12.6	14.9	15.4
14. Pirtz (Dworshak Dam)	12.5	58.2	32.5
15. Hansen and Harboe et al. (Canyon ferry Dam)	33.3	70.2	56.9
16. Russell and Burg (Water Tower Place)	15.7	19.3	31.5
17. Hanson	14.1	63.3	12.1
$\bar{\omega}_{all}$	23.6	58.1	35.0

In evaluating a creep and shrinkage model, it is important to avoid subjective bias. This has not been true of the evaluations of some other models recently presented in the literature. For example, consider that there are over 1,000 data points for creep durations under 100 days, and only 10 data points in excess of 1,000 days. If all these data were used in the statistical evaluation with the same weight, the error in predictions for times over 1,000 days would obviously have a negligible influence on the resulting statistics. Thus, a very low coefficient of variation of errors would be obtained if the model fitted the data well only in the range of up to 100 days. Yet predictions of the long-time behavior are most important.

A similar problem arises when the data bank has many values for loading ages under 100 days and very few over 1,000 days. However, in long-time relaxation, significant stress changes can occur in structures even after 1,000 days of age, and if the model does not predict the creep well for such large ages at loading, the stress relaxation cannot be correctly predicted from the principle of superposition. This point is important to realize since some recent comparisons with test data suffered from this kind of bias. Therefore one must ensure that the measured data within each decade of load or shrinkage duration (in logarithmic time scales) have equal weights. If possible this should also be ensured for the age at loading. Ideally, equal weights would be

Table 2.2: Coefficients of variation of errors (expressed as percentage) of shrinkage predictions of various models.

Model	B3	ACI	CEB
Test data	$\bar{\omega}$	$\bar{\omega}$	$\bar{\omega}$
1. Hummel et al.	27.0	30.0	58.7
2. Rüsch et al.(1)	31.1	35.2	44.8
3. Wesche et al.	38.4	24.0	36.1
4. Rüsch et al.(2)	34.7	13.7	27.8
5. Wischers and Dahms	20.5	27.3	35.9
6. Hansen and Mattock	16.5	52.9	81.5
7. Keeton	28.9	120.6	48.3
8. Troxell et al.	34.1	36.8	47.4
9. Aschl and Stökl	57.2	61.3	44.2
10. Stökl	33.0	19.5	29.6
11. L'Hermite et al.	66.7	123.1	69.4
12. York et al.	30.6	42.8	8.9
13. Hilsdorf*	11.7	24.7	29.6
14. L'Hermite and Mamillan	46.1	58.7	45.5
15. Wallo et al.	22.0	33.0	55.6
16. Lambotte and Mommens	39.1	30.7	31.3
17. Weigler and Karl	31.3	29.6	21.3
18. Wittmann et al.	23.7	65.4	40.0
19. Ngab et al.	20.4	45.3	64.6
20. McDonald	5.1	68.8	21.4
21. Russell and Burg (Water Tower Place)	38.5	51.0	58.1
$\bar{\omega}_{all}$	34.3	55.3	46.3

*Hilsdorf H.K., "Unveröffentlichte Versuche an der MPA München," private communication (1980).

achieved and subjective bias eliminated if the measured data had equal spacing in the logarithmic scales of load or drying duration and age at loading, and if they covered the entire range. But unfortunately creep measurements have not been made in this way.

In a previous studyß3,4, the subjective bias was eliminated by handsmoothing in log-time scale the experimentally measured curves and then placing points equally spaced in the log-scale on such hand-smoothed curves. However, there is a slight objection to this approach, since it inevitably involves some manipulation of test data and suppresses part (albeit only a very small part) of the scatter of data. A different approach has been adopted for the evaluation of Model B3. The data points in each decade in the logarithmic scale of load duration or drying duration are considered as one group, and each group of data points is assigned equal weight as a whole. Thus an individual data point in a particular group is weighed in

inverse proportion to the number of points in that group. Since most data sets have only few data points for load durations less than one day, all the data points for load durations under 10 days have been treated as part of one group.

As for the ages at loading, it turned out impractical to treat them in the same manner because very high and very low ages at loading are missing from most data. For this reason, statistical comparisons of Model B3 predictions with the values from the data bank have also been calculated separately for various decades of load duration and of ages at loading (grouped together in decades on the log-scale); see Table 2.5 for creep both without and with drying and Table 2.6 for shrinkage. (The coefficients of variation in this table could be used as the basis for a more refined statistical analysis of creep effects in structures, which would be more realistic than the simple use of the ω values in Eq. (1.26).)

A factor that contributes to the high value of scatter of shrinkage is the differences in the method of measuring shrinkage, which was not reported for many data. Some measurements have been made along the axis of the cylinder, others on the surface, and the base-length sometimes reached close to the ends of the specimen, sometimes not. Thus the complex deformation of specimen ends contaminated the results in an undocumented way. Another reason that the scatter of shrinkage is higher than that of creep is that the microcracking, which is very random, is more pronounced in shrinkage specimens than in compressed creep specimens.

It is worth noting that the coefficients of variation of Model B3 remain low even for the last decade of age at loading (over 1,000 days), while for some other models they become very large for that range. Correct representation of creep for loading ages over 1,000 days is important for calculating long-time stress relaxation from the principle of superposition, as well as for general solutions of stress variation in structures over long periods of time. In Table 2.6 for shrinkage, the coefficients of variation are not given separately for individual decades of the logarithm of the age t_0 at the start of drying because the effect of t_0 is relatively small.

It must be stressed that Fig. 2.1–2.4 are not intended as a verification of the model. For that purpose, the fits of all of the data sets in the data bank must be considered. Visual comparisons with all of the data sets have been generated by the computer but are too extensive for publication.

It should also be pointed out that the deviations from the data points seen in the figures are mainly caused by errors in the prediction of model parameters from the composition and strength of the concrete. If the model parameters are adjusted, all these data can be fitted very closely, but then one is not evaluating the prediction capability of the model. The figures showing most of the data from the data bank were presented in a previous paperß4 along with the basic information on the tests.

Other models in the literature have been verified by only a limited selection of the available test data. Before the age of computers this was understandable, due to the tediousness of such comparisons, but with the availability of a computerized data bank such selective comparisons with

Table 2.3: Coefficients of variation of errors (expressed as percentage) of the predictions of creep at drying for various models.

Model	B3	ACI	CEB
Test data	$\bar{\omega}$	$\bar{\omega}$	$\bar{\omega}$
1. Hansen and Mattock	5.8	32.1	11.9
2. Keeton	31.4	46.3	37.9
3. Troxell et al.	5.9	33.0	7.9
4. L'Hermite et al.	14.0	55.8	25.5
5. Rostasy et al.	6.5	20.9	14.8
6. York et al.	5.8	42.1	45.1
7. McDonald	10.9	40.4	38.9
8. Hummel	15.3	46.2	24.6
9. L'Hermite and Mamillan	20.6	62.5	15.2
10. Mossiossian and Gamble	11.3	71.7	30.8
11. Maity and Meyers	62.8	45.9	83.7
12. Russell and Burg (Water Tower Place)	10.7	41.2	19.1
13. Weil	23.9	42.1	30.2
14. Hilsdorf et al.	22.7	40.4	25.4
15. Wischers et al.*	22.3	44.3	17.4
16. Wesche et al.	28.1	38.6	24.0
17. Rüsch et al.	17.6	24.4	15.4
$\bar{\omega}_{all}$	23.0	44.5	32.4

* Data with curing duration less than one day are excluded.

test data are unjustifiable. There is always the danger of grossly distorting the results by a convenient selection of some test data sets to use for justifying some proposed model. For example, if among the 21 data sets used for shrinkage only the 12 most favorable data sets were selected (which might seem like plenty for justifying a model), the $\bar{\omega}_{all}$ value would be reduced from 34.3 to 23.7%. Likewise, if among the 17 data sets used for basic creep, only 7 of the most favorable of the data sets were selected, the $\bar{\omega}_{all}$ value would be reduced from 23.6% to 10.7%. These observations, and similar ones made inß3, document the dangerous deception that could be hidden in selective use of test data. Justifying some model by 12 or 7 data sets may look like plenty, yet it can be greatly misleading unless the data to be used for justification were chosen truly randomly.

If the aforementioned weights were not used, a smaller coefficient of variation of errors could be achieved. However, the fit of the long-time data would be much poorer. This fact clearly shows that the weights must be used in statistical evaluations. Better weighting, aside from applying sensitivity analysis to simplify the model, is one reason why the present coefficients of variation come out slightly higher than for the BP-KX Model.

A further assessment of the degree of scatter can be obtained from the

Table 2.4: Coefficients of variation of errors (expressed as percentage) of Model B3 predictions of the effect of constant elevated temperature on basic creep.

Test data	$\bar{\omega}$
1. Johansen and Best	20.3
2. Arthanari and Yu	35.5
3. Browne et al.	27.2
4. Hannant D.J.	14.0
5. York, Kennedy and Perry	41.1
6. Kommendant et al.	18.8
7. Okajima et al.	6.9
8. Ohnuma and Abe	23.7
9. Takahashi and Kawaguchi (a)	38.8
10. Takahashi and Kawaguchi (b)	43.9
$\bar{\omega}_{all}$	28.1

plots of measured value, X_k versus corresponding predicted values Y_k of creep and shrinkage ($k = 1, 2, 3...N_p$ are all the points in the plot). They are shown in Fig. 2.5, not only for the Model B3 but also for the previous ACI and the new CEB-FIP models. The basic creep and creep at drying are combined in the same plots.

If the models were perfect and scatter did not exist, these plots would be straight lines of slope 1. Thus deviations from this line represent errors of the model predictions plus inevitable scatter of the measurements. As seen, the errors of the Model B3 are significantly less than for the previous ACI 209 Model and distinctly less than for the new CEB Model. It should be noted that the Model B3 achieves the most significant improvements for large strains (or long times), which are most important. This is revealed by observing that the high strain points for the Model B3 lie relatively close to the line of slope 1, while those for ACI and CEB-FIP Models lie high above this line (which implies underprediction).

Table 2.5: Statistics of errors of various models for basic creep and creep at drying, calculated separately for different ranges of age at loading and creep duration (in days).

Model B3				
$\bar{\omega}$	$t' \leq 10$	$10 < t' \leq 100$	$100 < t' \leq 1000$	$t' > 1000$
$t - t' \leq 10$	17.8	24.0	19.8	
$10 < t - t' \leq 100$	13.7	23.1	25.3	29.3
$100 < t - t' \leq 1000$	13.9	20.5	22.6	33.6
$t - t' > 1000$	12.7	14.6	17.8	
ACI Model				
$\bar{\omega}$	$t' \leq 10$	$10 < t' \leq 100$	$100 < t' \leq 1000$	$t' > 1000$
$t - t' \leq 10$	60.3	30.7	33.3	
$10 < t - t' \leq 100$	45.7	36.7	49.9	97.1
$100 < t - t' \leq 1000$	34.6	39.9	51.7	93.9
$t - t' > 1000$	36.8	39.9	40.9	
CEB Model				
$\bar{\omega}$	$t' \leq 10$	$10 < t' \leq 100$	$100 < t' \leq 1000$	$t' > 1000$
$t - t' \leq 10$	40.5	23.1	11.2	
$10 < t - t' \leq 100$	25.8	23.5	21.2	40.8
$100 < t - t' \leq 1000$	17.5	22.8	25.0	41.3
$t - t' > 1000$	11.6	20.5	24.7	

Table 2.6: Statistics of errors of various models for shrinkage, calculated separately for different ranges of drying duration (in days).

$\bar{\omega}$	$t - t_0 \leq 10$	$10 < t - t_0 \leq 100$	$100 < t - t_0 \leq 1000$	$t - t_0 > 1000$
B3	38.5	29.3	22.4	19.6
ACI	67.8	50.4	43.3	44.8
CEB	53.5	40.2	44.7	37.4
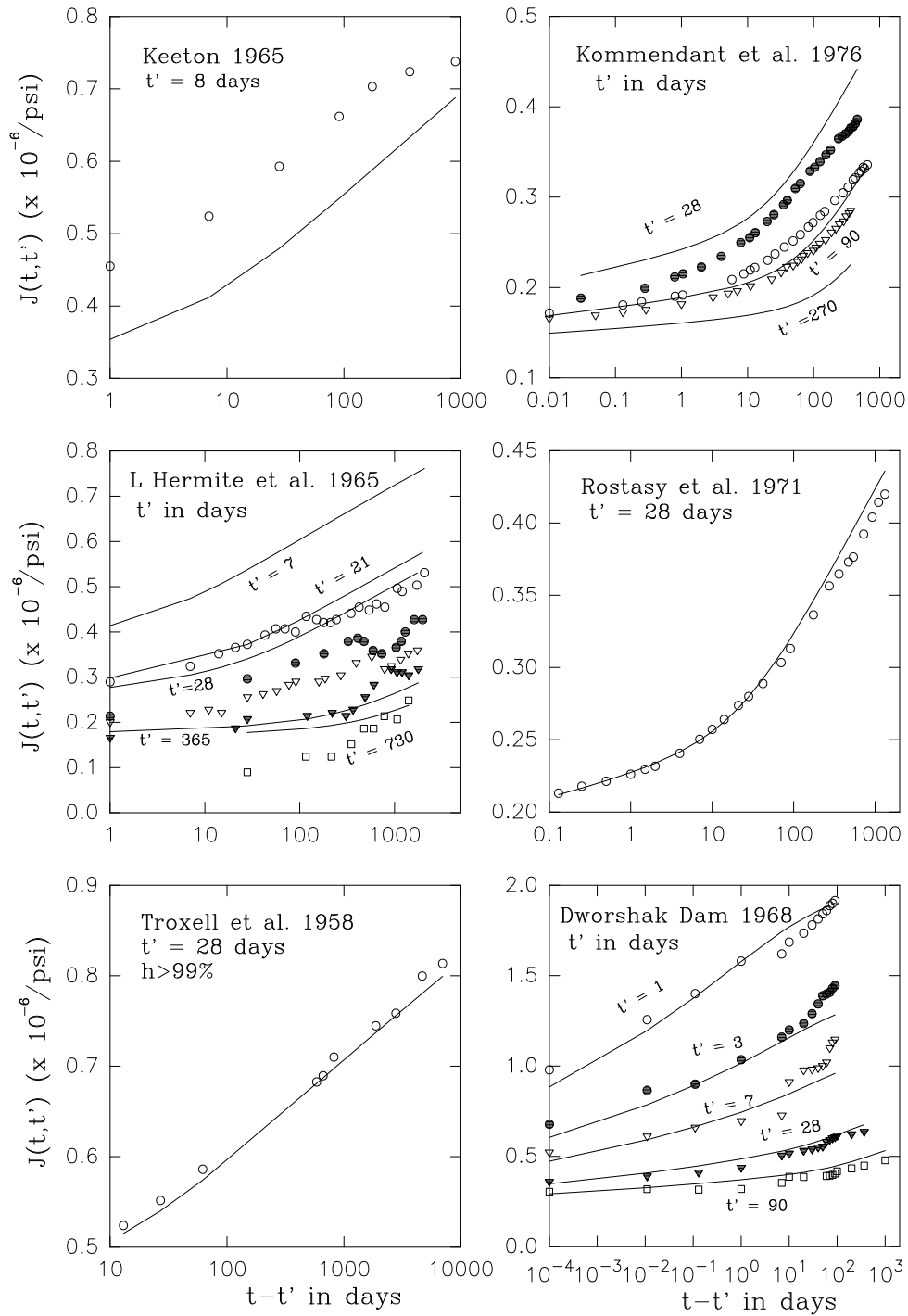
Figure 2.1: Comparison of the predictions of the Model B3 (solid lines) with some important test data for basic creep from the literature
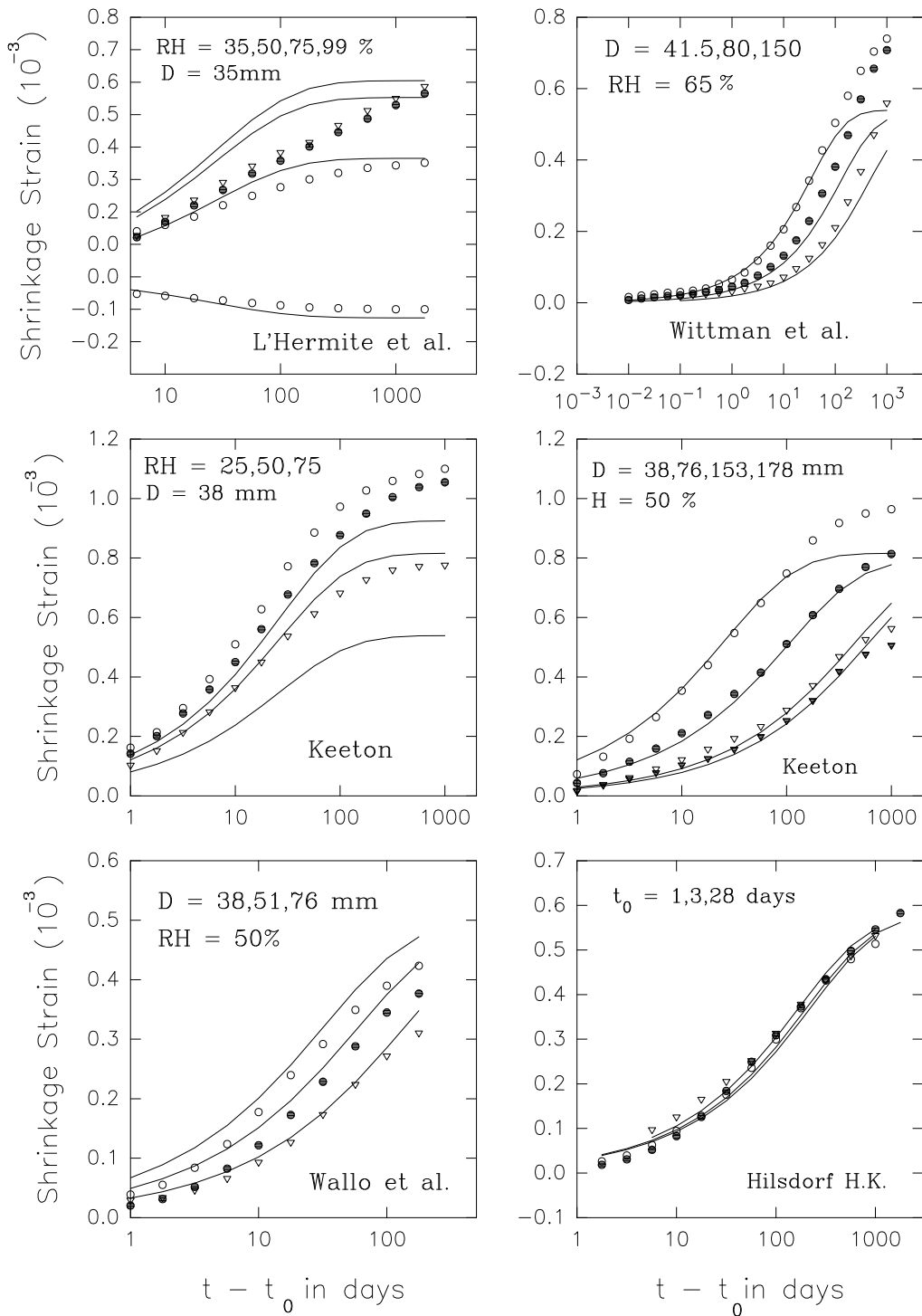
Figure 2.2: Comparison of the predictions of the Model B3 (solid lines) with some important test data for shrinkage from the literature
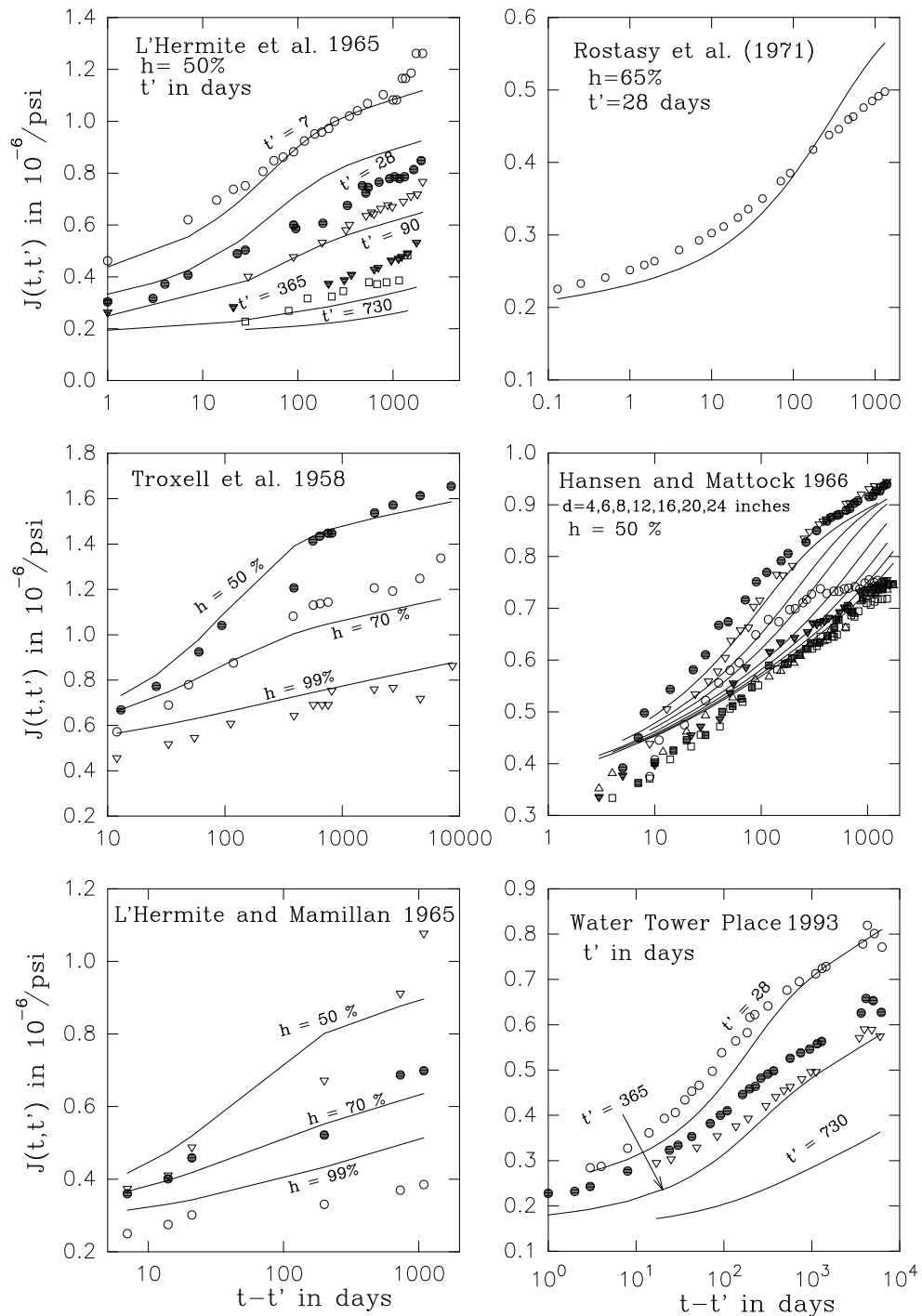
Figure 2.3: Comparison of the predictions of the Model B3 (solid lines) with some important test data for creep at drying from the literature
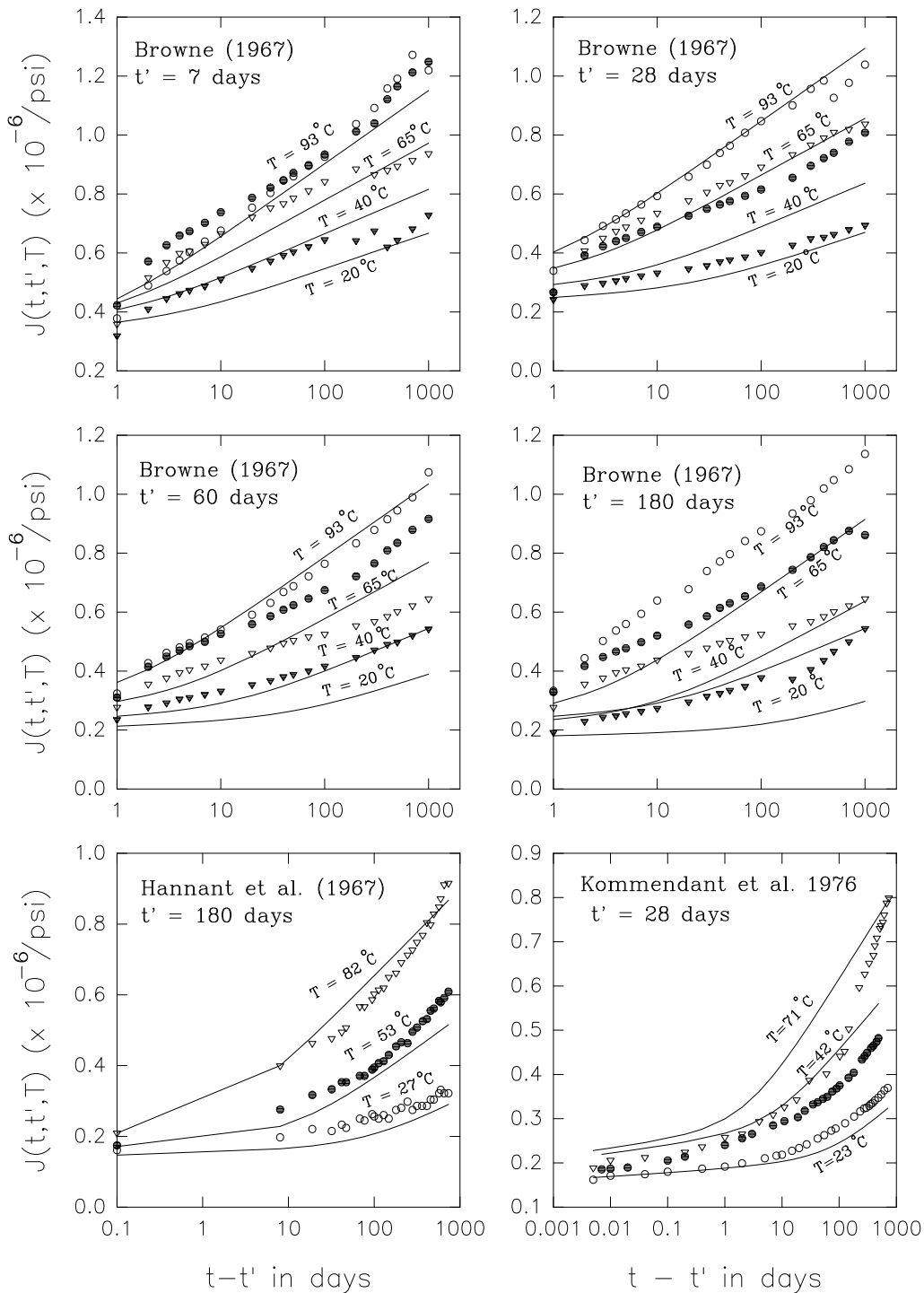
Figure 2.4: Comparison of the predictions of the Model B3 (solid lines) with some important test data from the literature for the effect of constant elevated temperature on basic creep

The correlation coefficient r of the population of the measured values and the corresponding model predictions is given in each figure. It has been calculated as $r = \sum_k (X_k - \bar{X})(Y_k - \bar{Y}/(N_p - 1)s_X s_Y$ where $s_X^2 = \sum_k (X_k - \bar{X})^2/(N_p - 1), s_Y^2 = \sum_k (Y_k - \bar{Y})^2/(N_p - 1), \bar{X} = \sum_k X_k/N_p, \bar{Y} = \sum_k Y_k/N_p$.

Note that r characterizes only the grouping of the data about the regression lines of the plots. The regression lines are also drawn in Fig. 2.5. But these regression lines do not have slope 1 and do not pass through the origin. This represents another kind of error that is not reflected in the value of r (this is the basic deficiency of this kind of plots compared to statistical regression). We see from these plots that in the case of Model B3, the regression line (dashed) is close to the line of slope 1 through the origin and also the value of r is close to 1.

The same plots of measured versus calculated values of creep and shrinkage are plotted in logarithmic scales in Fig. 2.6. These plots show the relative errors. As seen from these plots, especially for shrinkage, the relative error for all the models decreases with increasing shrinkage strain, as opposed to the absolute error seen in Fig. 2.5, which increases with increasing strain. These plots also show that the overall predictions are best for Model B3.

In the coordinates of Figs. 2.5 and 2.6 the strains for higher strength concretes are generally smaller than those for lower strength concretes. This is statistically undesirable because low strength concretes receive larger weights in such plots. To correct it we note that, roughly, the shrinkage and creep strains are proportional to $1/\sqrt{\bar{f}_c}$. Thus a plot of measured versus predicted values in which the coordinates are multiplied by $\sqrt{\bar{f}_c/5000}$ (strength values normalized by a mean strength of 5000 psi) gives roughly the same weight to concretes of high and low strengths. Such plots are shown in Fig. 2.7. From these plots it may be seen that the data which were crowded in Fig 2.5 have become more dispersed. The regression lines have been shown on these plots also and the correlation coefficient r has been calculated. In this case also the regression line for Model B3 is seen to be close to the line of slope 1 and the correlation coefficient r is also close to 1.

As mentioned in Chapter 1, the ACI formula for elastic modulus, $E = 57000\sqrt{\bar{f}_c}$ gives values approximately equal to $1/J(28+\Delta, 28)$ where $\Delta \approx 0.01$ day (or 5 to 20 min). This is verified by Fig. 2.8(a,b,c) which shows the values of $E_{28} = 1/J(28 + \Delta, 28)$ obtained in all the creep tests in the data bank for various Δ values.

In Fig. 2.8(d,e) two sets of short-time creep compliance data are plotted against $(t - t')^{0.1}$. We note that on such a plot the short-time creep curves appear as straight lines and that these straight lines corresponding to different ages at loading approximately meet at $t - t' = 0$. This demonstrates that the value of $q_1 = 1/E_0$ can be considered as age-independent. Fig 2.9 shows the values of $E_{28} = 1/J(28 + \Delta, 28)$ versus $\sqrt{\bar{f}_c}$ plotted for $\Delta = 0.01$ day. It can be seen that the discrepancy between the values of the ACI formula (line marked $E = 57000\sqrt{\bar{f}_c}$ in Fig. 2.9) and the values of $1/J(28.01, 28)$ is not large even though the method of measuring $E_{28} = 1/J(28.01, 28)$ in a creep test differs from the ASTM standards for measuring the elastic modulus.

45

The deviation of the regression line of the points in Fig. 2.9 indicates that a closer fit would be possible (with $E \propto \bar{f}_c^{2/5}$) but the improvement in creep predictions would be minor. The ACI formula, even though not optimal, is retained for the sake of uniformity.
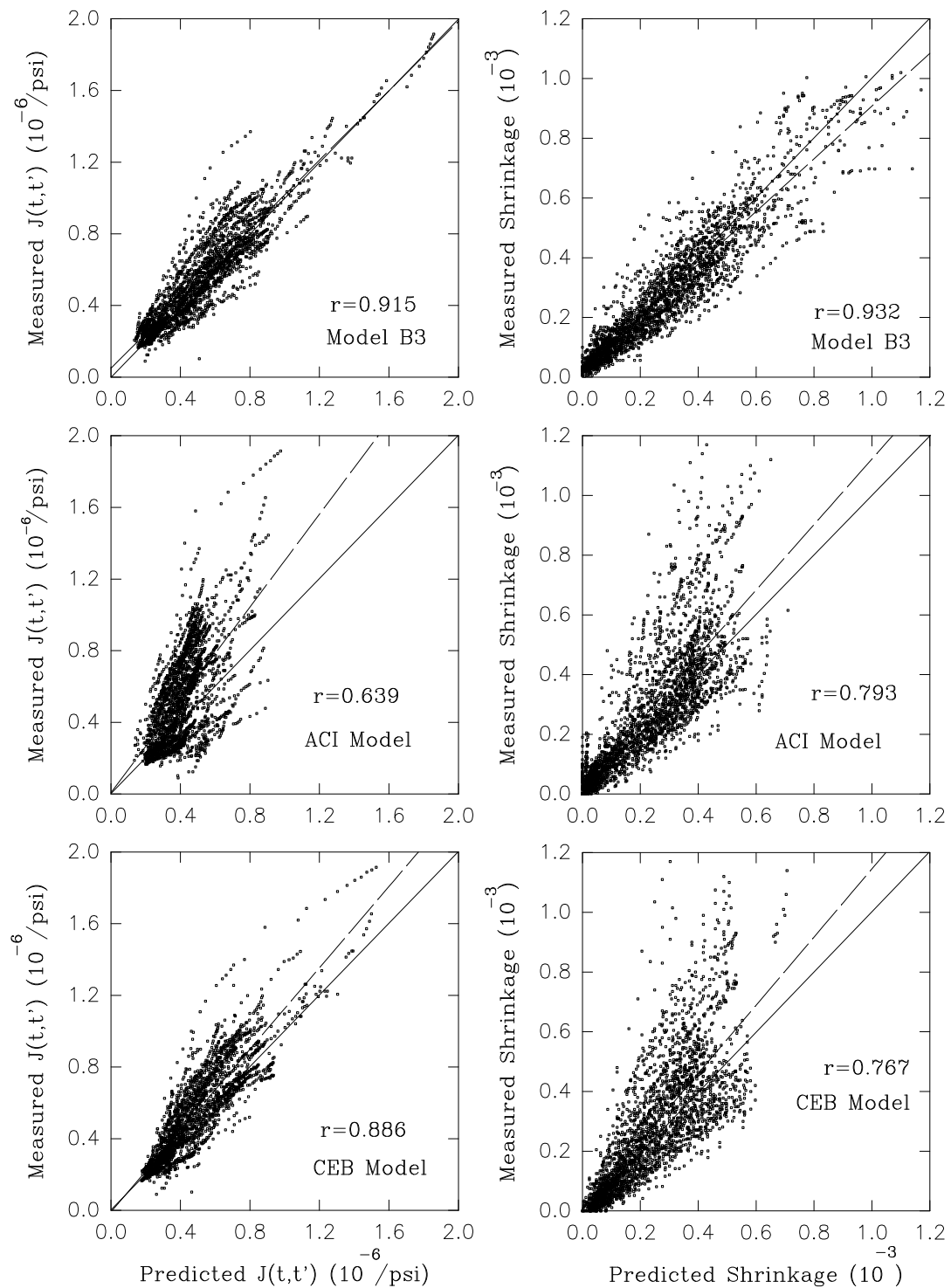
Figure 2.5: Scatter plots of the measured versus predicted values of creep and shrinkage (dashed lines are regression lines).
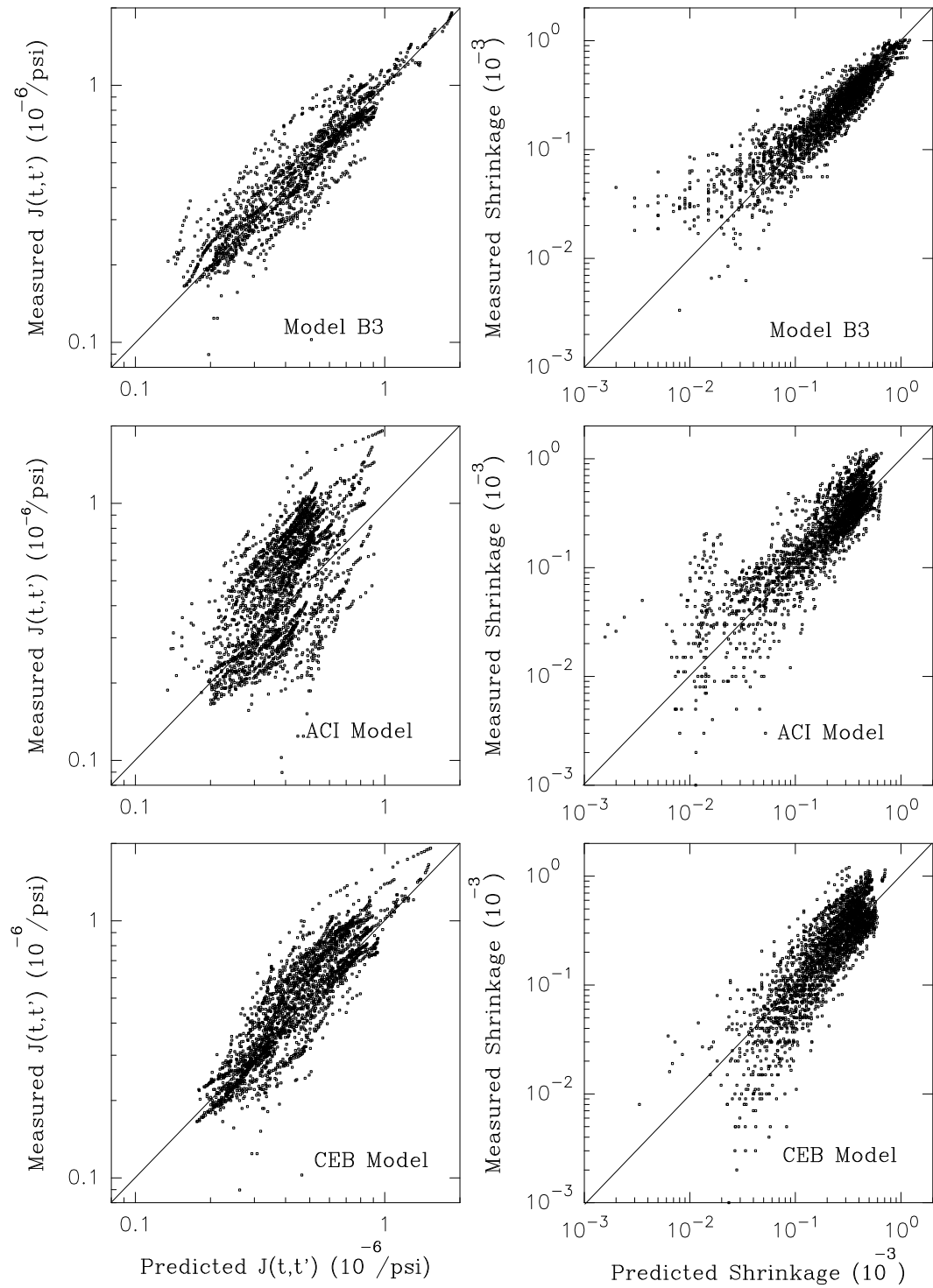
Figure 2.6: Scatter plots on logarithmic scales (showing relative error) of the measured versus predicted values of creep and shrinkage
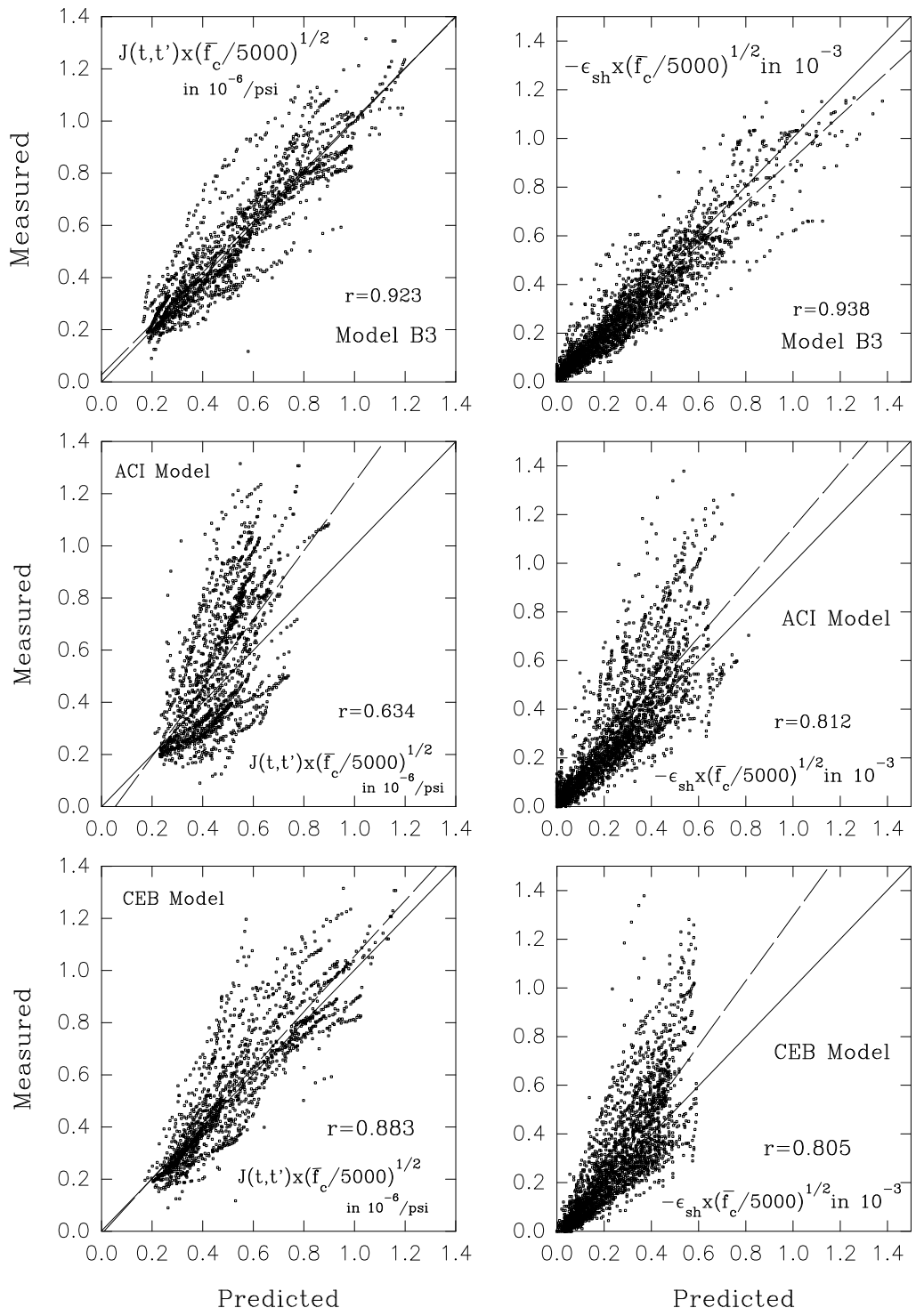
Figure 2.7: Scatter plots of the measured versus predicted values of creep and shrinkage with coordinates multiplied by $(\bar{f}_c/5000)^{1/2}$ (dashed lines are regression lines).
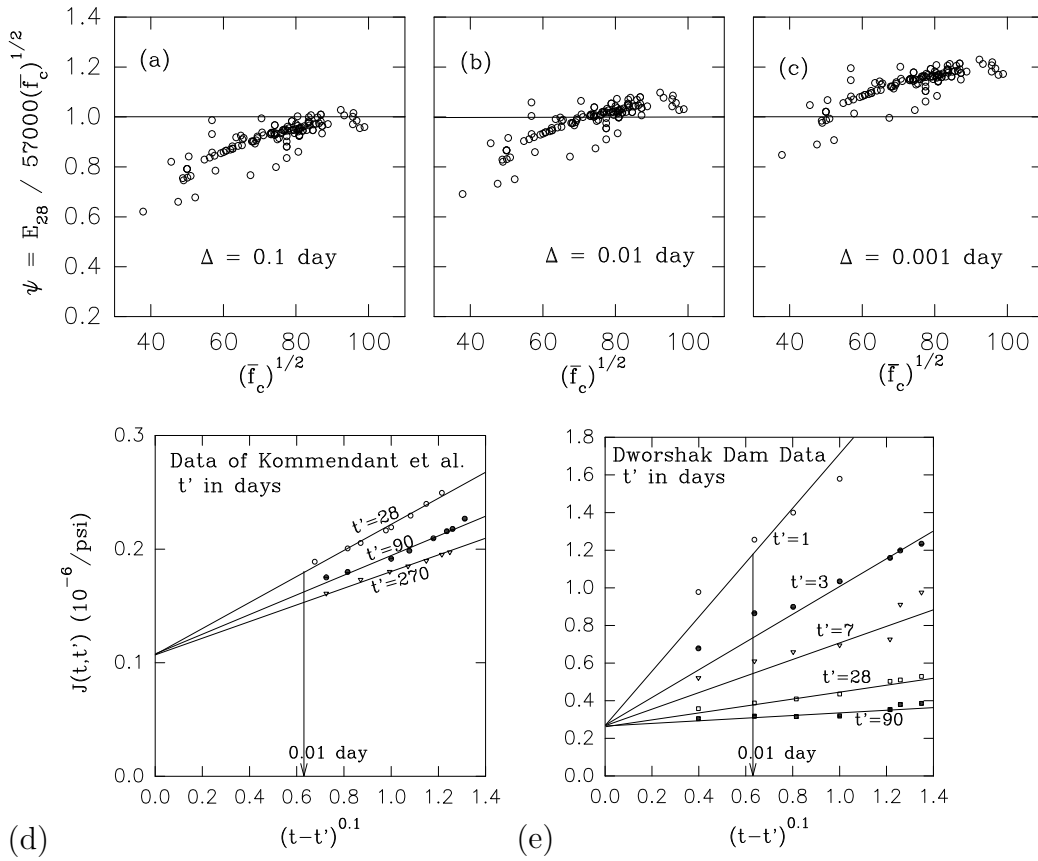
Figure 2.8: (a,b,c) Ratio of the values of $E_{28} = 1/J(28 + \Delta, 28)$, for various Δ values, to ACI formula for E; (d,e) Demonstration that the short-time creep data confirm the age-independence of $q_1 = 1/E_0$.

The age-dependence $E(t)$ according to Eq. (1.47) is similar to the ACI formula but not identical. For $\Delta = t - t' \ll t'$, one may replace t in Eq. (1.6) with t', and then one can easily integrate, obtaining:

$$J(t, t') = q_1 + (q_2 t'^{-1/2} + q_3) \ln[1 + (t - t')^n] + q_4 \ln \frac{t}{t'} \qquad (2.4)$$

where the last term is negligible for $t - t' \ll t'$ or $t \approx t'$. Using this in Eq. (1.46) one gets Eq. (1.47) which yields the solid curves in Fig. 2.10. Also shown in this figure are the curves of the ACI formulaß5 $E(t) = E(28)[t/(\alpha + \beta t)]^{1/2}$, as well as the test results of Shidelerß45. We see the present formulation actually fits these data better than the ACI formula (ACI 209ß5), particularly for long times,[†] but the difference is not significant.

[†]This comparison study was done by Anders Boe Hauggaard, visiting research scholar at Northwestern University from the Technical University of Denmark.
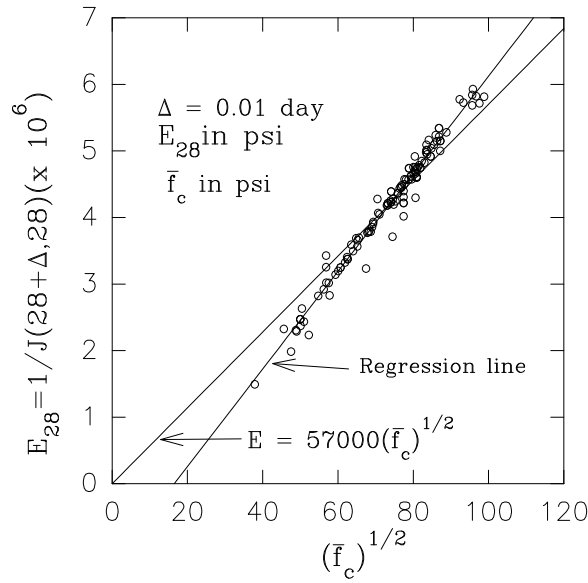
Figure 2.9: Elastic modulus predictions by creep formulae

2.3 Updating of Creep and Shrinkage Predictions Based on Short-Time Measurements

The updating of creep predictions based on short-time measurements has already been discussed in Chapter 1, but further discussion of the updating of shrinkage predictions is in order.

The updating of shrinkage predictions as well as creep predictions is best handled by the Bayesian statistical approachß11,12. However, for the sake of simplicity, this approach is avoided here, although Bayesian extension of the present analysis would be possible.

2.3.1 Problems in Updating Shrinkage Predictions

The problem of updating is much harder for shrinkage than for creep because of the recently discovered ill-posedness of the shrinkage updating problemß13. The updating based only on short-time measurements of shrinkage values is not possible unless the measurements extend into the final stage in which the shrinkage curve begins to level off on approach to the final value. Before reaching this final stage, it is impossible to tell, without additional information, how much longer the curve of ϵ_{sh} versus $\log(t - t_0)$ will rise at non-decreasing slope and when it will start to level off.

If the time range of shrinkage measurements is not sufficiently long, the problem of fitting the shrinkage formula in Eq. (1.8)–(1.9) to the measured strain values is what is known in mathematics as an ill-posed problem. In other words, very different values of parameters $\epsilon_{sh\infty}$ and τ_{sh} can give almost equally good fits of short-time data, as documented in Fig. 2.11(a,b). This
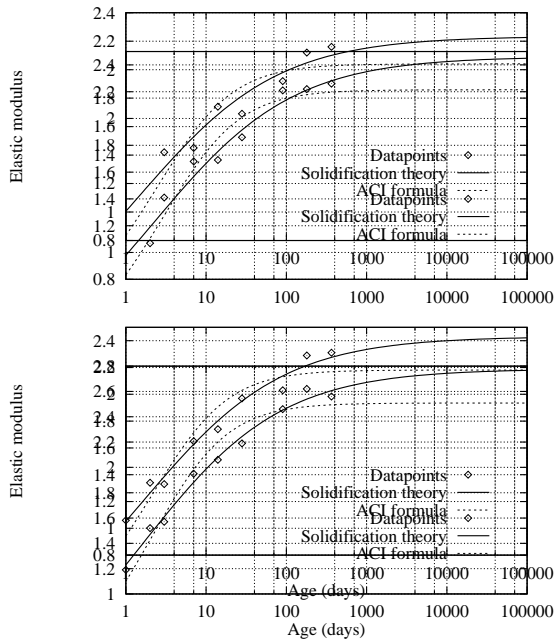
Figure 2.10: Comparison of the ACI formula and Eq. (1.47) for the age-dependence of elastic modulus (given in 10^{-6} psi in this figure)

is true not only for the present Model B3 formulae but also for all other realistic shrinkage formulae, including the Ross' hyperbola used in the 1971 ACI Model (this formula does not give a good shape of the shrinkage curves and disagrees with the asymptotic forms for short and long times required by the RILEM Committee Guideliness26). The problem is clear from Fig. 2.11, in which two shrinkage curves according to the present model or the ACI Model (ACI 209), corresponding to very different parameter values, are shown to nearly coincide for a long period of time. If the data do not reach beyond the time at which the two curves shown in Fig. 2.11(a,b) begin to significantly diverge, there is no way to determine the model parameters unambiguously.

Fig. 2.11c underscores the point that comparisons of shrinkage measurements of different concretes can be misleading if the test durations are not long enough. Shrinkage time curve a corresponds to a relatively porous concrete that dries quickly and reaches moisture equilibrium soon but has a low final shrinkage. Curve b corresponds to a dense concrete which dries very slowly but has a large final shrinkage. However, a short-time shrinkage test, terminating at the points marked, would show concrete a to have a higher final shrinkage than concrete b, which is not true.

¿From such plots it is concluded that a reliable determination of the final value of shrinkage would require, for 6 in. (15 cm) diameter cylinders, measurements of at least five years in duration, which is unacceptable for a designer. Even with a 3 in. (7.5 cm) diameter cylinder, this would exceed
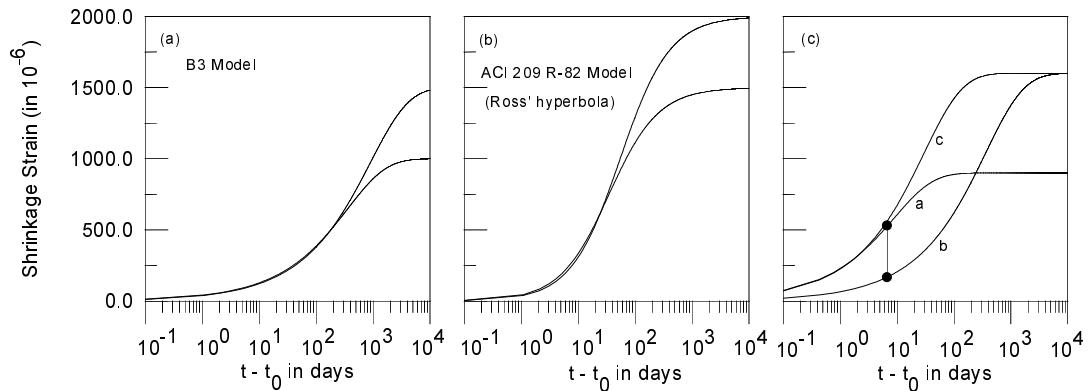
Figure 2.11: Examples of shrinkage-time curves giving nearly the same initial shrinkage but very different final values. (a): Model B3, (b): ACI 209 Model (all other realistic expressions for shrinkage also exhibit such behavior) and (c) Possible shrinkage-time curves of identical specimens of different concretes

15 months. Increasing the temperature of the shrinkage tests to about 50° C would not shorten these times drastically and would raise further uncertainties due to the effect of temperature. A greater increase of temperature would change the shrinkage properties so much that inferences for the room temperature would become questionable. Significant acceleration of shrinkage would require reducing the thickness of the shrinkage specimen under about 1 in. (2.54 cm). But in that case the specimens would have to be saw-cut from larger specimens and this would cause the three-dimensional composite interaction between the mortar matrix and the aggregate pieces to be very be different from bulk concrete. Thus, for shrinkage updating from short-time tests, some further information (e.g. an estimate of the final water loss, used in the following updating procedure) is essential, in addition to the short-time test data.

53

2.3.2 Updating Shrinkage Prediction when τ_{sh} Is Known

The nonlinear parameter in the shrinkage model is τ_{sh}. So let us first describe the updating assuming that the value $\bar{\tau}_{sh}$ of shrinkage half-time τ_{sh} has somehow been determined by short-time measurements. The updated values of shrinkage prediction may be written as $\epsilon^*_{sh}(t, t_0) = p_6 \bar{\epsilon}_{sh}(t, t_0)$ (Eq. (1.33)) in which $\bar{\epsilon}_{sh}(t, t_0)$ are the values predicted from Model B3 based on $\bar{\tau}_{sh}$, ignoring Eq. (1.11) for τ_{sh}, and p_6 is an update parameter to be calculated. Consider that values ϵ'_{sh_i} at times t_i have been measured. The optimum update should minimize the sum of squared deviations Δ_i of the updated model from the data; that is

$$S = \sum_i \Delta_i^2 = \sum_i (p_6 \bar{\epsilon}_{sh_i} - \epsilon'_{sh_i})^2 = \text{Min} \tag{2.5}$$

where $\bar{\epsilon}_{sh_i} = \bar{\epsilon}_{sh}(t_i, t_0)$. A necessary condition of a minimum is that $dS/dp_6 = 0$. This yields the condition $\sum_i (p_6 \bar{\epsilon}_{sh_i} - \epsilon'_{sh_i}) \bar{\epsilon}_{sh_i} = 0$. From this, the value of the update parameter is calculated as $p_6 = \sum_i \bar{\epsilon}_{sh_i} \epsilon'_{sh_i} / \sum_i \bar{\epsilon}_{sh_i}^2$, which is Eq. (1.32).

2.3.3 Measuring Water Loss to Update Shrinkage Prediction

Second consider how τ_{sh} can be estimatedß2. To circumvent the aforementioned ill-posedness of the shrinkage updating problem (Fig. 2.11a,b), the following approach has been proposed in Ref. 2. It has been known for a long time that shrinkage strains are approximately proportional to the water loss, denoted as Δw. The idea is that: (1) water loss can be easily measured simultaneously with shrinkage tests, and (2) the final value $\Delta w_\infty(0)$ of water loss at nearly zero environmental humidity can be easily estimated by heating the test specimen in an oven to $110°$ C right after the short-time test is terminated. Although such heating causes a slightly higher water lossß46 than drying up to hygral equilibrium at constant temperature and at $h \approx 0$, the difference can be neglected.

As another spoiling influence, one might point out carbonation of $Ca(OH)_2$, which occurs fast upon heating and increases the weight of the specimen. But, because of the time the diffusion of CO_2 requires, this effect is probably significant only on thin cement paste specimens. Thus the sum of the weight losses during shrinkage and the subsequent heating can be assumed to be approximately equal to the final weight loss $\Delta w_\infty(0)$ that a shrinkage specimen would experience if it attained hygral equilibrium at $h \approx 0$.

To estimate the final water loss $\Delta w_\infty(h)$ for shrinkage humidity h, we need an approximation for the desorption isotherm. Assuming that the shrinkage is proportional to water loss, this isotherm should approximately be a linear expression in function h^3 used in k_h in Eq. (1.10). Although the shapes of the desorption isotherms of concrete vary considerablyß47-49, the following expression seems reasonable (Fig. 2.12): $\Delta w_\infty(h) \approx 0.75 \left[1 - (h/0.98)^3 \right] \Delta w_\infty(0)$, valid for $0.25 \leq h \leq 0.98$ (which is Eq. (1.30) of Chapter 1). It satisfies the condition that there is no water loss for $h \approx 0.98$ (in water immersion, i.e.

for $h = 1.0$, there is water gain). For $h < 0.25$ this expression (Fig. 2.12) is invalid, but environmental humidities below 25% are normally not of interest.
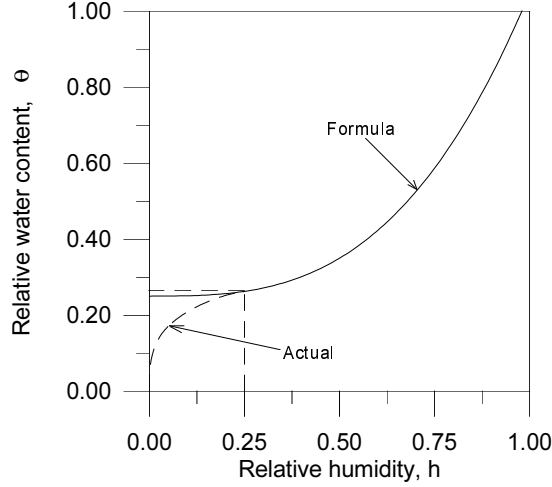

Figure 2.12: Relative water content, $\theta = 1 - \Delta w_\infty(h)/\Delta w_\infty(0)$, vs. relative humidity, h

An alternative way to estimate $\Delta w_\infty(h)$ might be to estimate first the final degree of hydration in the shrinkage specimen and on that basis calculate the final water content from the total water content and cement content in the mix. Sealed curing (rather than curing in a water bath) would be required to prevent imbibition of water before the shrinkage test. However, the uncertainty involved in that approach would no doubt be higher.

Because Eq. (1.8) and (1.9) were derived from diffusion theory, under the assumption of proportionality to water loss, the evolution of water loss with time should approximately follow the same equation as Eq. (1.9) in Chapter 1, that is,

$$\frac{\Delta w}{\Delta w_\infty(h)} = \tanh \sqrt{\frac{t - t_0}{\tau_{sh}}} \tag{2.6}$$

where Δw is the weight loss of the shrinkage specimen up to time t. This equation can easily be rearranged to a linear form: $t - t_0 = \tau_{sh}\psi$, with $\psi = \left[\tanh^{-1}(\Delta w/\Delta w_\infty(h))\right]^2$, which appears in Eq. (1.31).

Now consider that, at times t_i of shrinkage measurements, the values of water loss Δw_i up to times t_i have also been measured and the corresponding values of ψ_i have been calculated. The optimum value of τ_{sh} must minimize the sum of square deviations, i.e.

$$S = \sum_i [\tau_{sh}\psi - (t_i - t_0)]^2 = \text{Min} \tag{2.7}$$

A necessary condition of a minimum is that $dS/d\tau_{sh} = 0$. This yields the linear equation $\sum_i [\tau_{sh}\psi_i - (t_i - t_0)]\psi_i = 0$, from whichß2: $\tau_{sh} = \sum_i(t_i -$

$t_0)\psi_i / \sum_i \psi_i^2$ which is Eq. (1.32). Based on this value, one may then use Eq. (1.33) to obtain the updating parameter p_6 for the final shrinkage value.

In the foregoing procedure based on Ref. 2, it has been assumed that shrinkage half-time, $\tau_{sh} = 1.25\tau_w$, where τ_w = the water-loss half-time. Fitting of the shrinkage and water loss data for very thin cement paste specimensß47 has shown τ_{sh} to be somewhat higher than τ_w. Similar results were obtained from the data for six different concretes used in French nuclear containments, which provided $\tau_{sh}/\tau_w = 1.30$ for power plant Penly, 2.23 for Chooz, 1.28 for Civaux(BHP), 1.32 for Civaux(B11), 0.55 for Flamanville, 1.06 for Paluelß14. The average ratio is $\tau_{sh}/\tau_w \approx 1.25$, which explains Eq. (1.32). The reason for $\tau_{sh} > \tau_w$ may be explained by the fact that the microcracking in the surface layer of drying specimens accelerates water loss but decreases average axial shrinkage in the cross-section. Another reason could be the existence of a certain time-lag caused by the local microdiffusion of water from gel micropores to capillary pores.

It must be emphasized that a systematic check of the proposed procedure for estimating the final water loss by heating, has not yet been made. Also a more systematic verification of the assumption that $\tau_{sh} \approx 1.25\tau_w$ is desirable. This new method deserves deeper evaluation of its accuracy.

The ill-posedness of time extrapolation of course occurs also for the portion of creep due to drying, because, being governed by diffusion phenomena, it is based on the same function τ_{sh}. Even though this is a lesser problem (because only part of creep is affected), it is advisable to eliminate this ill-posedness in extrapolation from short-time data. To do that one should use the τ_{sh} value obtained from the water-loss data for the function $F(t, t')$, in Eq. (1.28), which is used in extrapolation of creep instead of using the τ_{sh} value from the prediction formula in function $F(t, t')$.

2.3.4 Importance of Measuring the Initial Shrinkage and Data Correction

Theoretically, the shrinkage curve after the surfaces dries should initially evolve in proportion to $\sqrt{t - t_0}$ if the exposure to environment is suddenß50. This is, for example, quite well verified by the data reported by Wittmann, Bažant and co-workersß35. However, some shrinkage data, especially older ones, do not quite agree with this rule. The most likely reason is that the first reading was not taken right at the time of stripping of the mold, which means that some initial shrinkage strain $\Delta\epsilon_{sh}$ has been missed. Thus, the erroneous readings $\tilde{\epsilon}_{sh}$ should be corrected by constant $\Delta\epsilon_{sh}$. Neglecting other possible influences, this may be done by optimally fitting to the initial data points the relation: $\tilde{\epsilon}_{sh} + \Delta\epsilon_{sh} = k\sqrt{t - t_0}$, in which k is some constant. This relation can be represented by a linear regression in the plot of $\tilde{\epsilon}_{sh}$ versus $\sqrt{t - t_0}$.

Another error may occur when the seals leak moisture during the curing before the shrinkage test. This may cause $\Delta\epsilon_{sh}$ to come out negative. But no correction to data is possible in this case. Such data should be discarded if $|\Delta\epsilon_{sh}|$ is large. In the present data sets, these corrections have been found to be relatively small and at the same time quite uncertain in most cases, due

to the high initial scatter of the data. Therefore, these corrections have not been used in the optimum fitting of Model B3. Such corrections, however, could be important for the evaluation of short-time data with the purpose of extrapolating for longer times.

2.3.5 Extension to Special Concretes

Special concretes such as high-strength or fiber-reinforced concretes contain various admixtures and pozzolanic materials. Experimental research has indicatedß28,29 significant influence of these additives on creep and shrinkage (for a detailed review see the report of subcommittee 5 of ACI 209, chaired by J.J. Brooks). Parameter prediction formulae based on composition are, for such concretes, difficult to formulate because of the wide variety of additives used. However, Model B3 can be applied to such special concretes if the material parameters are calibrated by short-time tests, provided that certain special behavior is taken into account.

The observed autogenous shrinkage, which is very small for normal concretes, represents a significant portion of the total shrinkage in high-strength concretesß51. The reason is that, because of small ratios of water to cementitious materials, significant decrease of pore humidity due to self-desiccation occurs in such concretes. Despite limited test dataß51, the following formula can be recommended for the total shrinkage of high strength concretes:

$$\epsilon_{sh}^{total}(t, t_0) = \epsilon_a(t) + \epsilon_{sh}(t, t_0) \tag{2.8}$$

where ϵ_a is the autogenous shrinkage, and ϵ_{sh} is the drying shrinkage. The autogenous shrinkage can be approximately described by the formula:

$$\epsilon_a(t) = \epsilon_{a\infty}(0.99 - h_{a\infty})S_a(t); \qquad S_a(t) = \tanh\sqrt{\frac{t - t_s}{\tau_a}} \tag{2.9}$$

where t_s is the time of final set of cement; ϵ_{sh} is the same as given by Eq. (1.8); τ_a is the half-time of autogenous shrinkage, which depends on the rate of hardening of the type of high-strength concrete; and $h_{a\infty}$ is the final self-desiccation humidity (it may be assumed to be about 80% because hydration almost ceases below this humidity). Note that there is no size or shape effect in the above formula because self-desiccation is not caused by diffusion of water (except that the non-uniform heating due to the rapid hydration reaction during autogenous shrinkage can induce moisture diffusion and some associated size effect, but this is neglected here). The material parameters in the foregoing formula may be calibrated by carrying out shrinkage measurements on sealed specimens (autogenous shrinkage) and drying specimens (total shrinkage). The autogenous shrinkage measured on high-strength concrete tends to terminate early. After self-desiccation, there is not much water left in the specimen for drying by diffusion because the water contents of high-strength concretes tend to be small.

2.4 Theoretical Justifications of Model B3

2.4.1 New Theoretical Formula for Drying Creep

The formula used for drying creep in the preceding BP and BP-KX Models was semi-empirical. A more rational formula, presented in Eq. (1.14), has been derived theoretically as followsß2.

We assume that the additional creep due to drying is essentially the stress induced shrinkage, that is, we neglect the complex and hard to quantify influence of cracking. Note that because creep is tested under compression, the effect of microcracking is reduced. But even if it were considered, the basic aspect of the following derivation (especially, the role of τ_{sh}) would still apply because the microcracking is also associated with water diffusion. (For the theoretical background of the drying creep problem, seeß20,22,26)

According to ß22, the average rate of the stress-induced shrinkage within the cross section may be approximately expressed as $\dot{C}_d = \kappa \dot{H}$ in which H is the spatial average of pore relative humidity over the cross section and κ is a coefficient. This coefficient may be considered as a function of H as well as the total stress-induced strain C_d. We assume the following relation:

$$\dot{C}_d(t, t', t_0) = \frac{k\rho(H)}{C_d}\dot{H} \tag{2.10}$$

where ρ is a coefficient depending on H, and k is a constant. This can be rewritten as $d(C_d^2)/dt = 2k\rho(H)k\dot{H}$. Integrating from age at loading t' to the current time t,

$$C_d^2 = 2k \int_{t'}^{t} \rho(H)\dot{H}d\tau = 2k \int_{H(t')}^{H(t)} \rho(H)dH \tag{2.11}$$

Since drying creep, like shrinkage, is caused by water content changes governed by the diffusion theoryß50, the following equation gives a good approximation (having the correct asymptotic forms for very short and very long times $t - t_0$):

$$H(t) = 1 - (1 - h)S(t) = 1 - (1 - h)\tanh\sqrt{\frac{t - t_0}{\tau_{sh}}} \tag{2.12}$$

Here $S(t)$ is given by Eq. (1.9). According to diffusion theory, the water loss from the specimen is initially (for small $t - t_0$) proportional to the square root of drying time. Eq. (2.12) satisfies this property because, for $t - t_0 \ll \tau_{sh}, 1 - H = (1 - h)[(t - t_0)/\tau_{sh}]^{1/2}$. For long times $t - t_0 \gg \tau_{sh}$, Eq. (2.12) approaches the final asymptotic value exponentially, as required by the diffusion theoryß50.

Studies of the data show that the function $\rho(H)$ may be assumed approximately in the form $\rho(H) = e^{aH}$. Evaluation of the integral in Eq. (2.11) then yields:

$$C_d^2 = 2k \left[e^{aH(t)} - e^{aH(t')} \right] \tag{2.13}$$

which is the expression used in Eq. (1.14).

2.4.2 Basic Creep and Shrinkage

The theoretical justification of the formulae used in Model B3 is the same as stated inß4 for the previous BP-KX Model and for some formulae inß3. Briefly, Eq. (1.6) is derived from the solidification theoryß6,52 in which it is assumed that the chemical constituents of cement paste are not aging and the aging is exclusively due to volume growth and the interlinking of layers of a non-aging constituent of viscoelastic properties.

In the previous simplified version of this modelß13, the present formula for basic creep was replaced by the log-double power law, which is simpler. However, it is not much simpler and gives poor long time predictions for concrete loaded at a very young age. Also, the log-double power law (as well as the current compliance function in ACI 209 and many other compliance functions proposed in the past) is not entirely free of the problem of divergence identified in previous worksß1. This, for example, means that these other models can give, according to the principle of superposition, non-monotonic creep recovery curves (i.e. reversal of recovery). Furthermore, the calculation of relaxation function $R(t, t')$ from the solidification theory compliance function does not give negative values of $R(t, t')$ while for the other compliance functions (log-double power law, ACI 209) negative values of $R(t, t')$ are obtained for large t and small t'. In addition, the solidification theory does not violate thermodynamic restrictions with respect to the aging effect on material stiffness, whereas the other theories do. Because of these advantages the formulation based on solidification theory is preferred. It also gives better data fits.

Eq. (1.9) for the time function of shrinkage represents the simplest possible interpolation between two required asymptotic behaviors. For short times the shrinkage strain (as well as the weight loss) should evolve as the square root of the drying duration, and for long times the differences from the final value should decay as an exponential.

Eq. (1.9) is also justified by diffusion theory, which requires the shrinkage half-time to scale as D^2. Here a remark on moisture diffusivity in concrete and its effect on evolution of shrinkage is in order. Although k_t in Eq. (1.11) has the dimension of the inverse of diffusivity, it represents the diffusivity of moisture only partly. Eq. (1.11) together with Eq. (1.13) also includes the effect of microcracking, which tends to reduce long-term shrinkage value and at the same time accelerates the shrinkage growth for medium durations (by increasing the diffusivity). The diffusivity, of course, must be expected to increase with w/c (or with $1/f'_c$) and decrease with t_0, but these trends are offset by the effects of Eq. (1.13) on shrinkage evolution.

Like shrinkage, the drying creep, too, must depend on D, which is ensured by the dependence of τ_{sh} on D in Eq. (1.11). This causes the drying creep of a very thick specimen to be negligible within normal lifetimes of structures; the total creep approaches basic creep for $D \to \infty$.

Eq. (1.13) for $\epsilon_{sh\infty}$ is justified by the fact that drying shrinkage is caused mainly by forces applied on the solid microstructure as a result of tension in capillary water and adsorbed water layers. According to this mechanism, the shrinkage should decrease with increasing elastic modulus. Because the

growth of elastic modulus continues longer in thicker cross sections (due to slower drying), the decrease of $\epsilon_{sh\infty}$ for thicker cross sections should be more pronounced and of longer duration.

2.4.3 Role of Environmental Fluctuations

Some engineers are skeptical about laboratory tests conducted at constant environmental humidity. They suspect such tests to have little relevance to structures exposed to weather of fluctuating relative humidity. This view, however, is unjustifiably pessimistic. Although there is a certain effect (and it is known how to take it into account–see the model for creep at cyclic humidity and temperature inß3 andß4), analysis of moisture diffusion indicates that, for not too thin cross-sections, the effect of such fluctuations cannot be very large and cannot invalidate the present model. Diffusion analysis shows that for normal concretes a periodic component of environmental humidity history $h(t)$ having a period T_h does not affect the pore humidity at the center of the cross-section if $\tau_{sh} \geq 2T_h$ or for normal concretes

$$D \geq \sqrt{\frac{T_h}{10 \text{ days}}} \quad \text{in.} \tag{2.14}$$

This means that for $D > 6$ in., the annual humidity cycles do not affect the center of a wall 6 in. thick. Furthermore, one calculates that these humidity cycles affect less than 10% of the cross-section thickness when D is about 3 times larger than that calculated by Eq. (2.14), i.e., $D > 18$ in. For high-strength concretes, which are much less permeable, these limits for D are much smaller. Normal cracking cannot diminish these limits for D significantly (as indicated by measurements of the drying diffusivity of concrete with thin cracksß53).

On the other hand, for the fluctuating component of temperature, the aforementioned limits for D are much larger, because in concrete the heat diffusivity is about 100 times higher than drying diffusivity. But the effect of temperature on shrinkage and creep is considered secondary and is ignored in present design practice. Nevertheless, the effect of temperature deserves deeper study.

2.5 Concluding Comments

Model B3 (based on the third update of the creep and shrinkage predictions models developed at Northwestern University) is simpler than the previous versions, gives good agreement with available test data, is validated by a larger test set of test data, and is better justified theoretically on the basis of the understanding of the mechanisms of creep and shrinkage. Simplification of the effect of concrete composition and strength has been achieved mainly by systematic sensitivity analysis of the parameters of the model. Theoretical improvement has been achieved by a simplified integration of the previously established formulation for stress-induced shrinkage.

The coefficients of variation of the errors of the prediction model are determined on the basis of the RILEM data bank which originated from a previous ACI-RILEM data bank. They should serve as the basis for statistical analysis of creep and shrinkage effects in structures, making it possible to determine suitable confidence limits (such as 95% confidence limits) rather than average properties.

A method of updating the main parameters of the model on the basis of limited short-time tests is presented. Difficulties with ill-posedness of the updating problem for shrinkage are circumvented by a new method exploiting simultaneous short-time measurements of water loss during shrinkage. Such updating can significantly reduce the uncertainty of prediction, and is particularly important for extensions to high strength concrete with various admixtures, superplasticizers, water-reducing agents and pozzolanic materials.

2.6 Appendix to Chapter 2: Sensitivity Analysis

The formulae in (1.17) and (1.19) for predicting Model B3 parameters from concrete composition and strength are simpler than those in the previous models. The simplification has been achieved mainly through sensitivity analysisß53,54. First, all the parameters of the model are assumed to depend on all the composition and strength parameters, in the form of products of power functions (which means that the logarithms of these parameters are assumed to depend linearly on the logarithms of composition parameters and of strength). Then the parameter values are optimized for the entire data bank. In the case of basic creep, the following expressions are thus obtained:

$$q_2 = 0.77(c)^{0.73}(a/c)^{-0.09}\left(0.001\bar{f}_c\right)^{-1.25}, \quad q_3 = 0.36(w/c)^5 q_2 \qquad (2.15)$$

$$q_4 = 0.001(c/30)^{3.57}\left(0.001\bar{f}_c\right)^{1.29}(a/c)^{3.16} \qquad (2.16)$$

Then the plots of the model parameters versus the composition and strength parameters over their typical ranges are considered; see Fig. 2.13. In this figure the strength and composition parameters are normalized by dividing by their maximum value. As seen from this figure, various model parameters are almost insensitive to some of the composition and strength variables (see the nearly horizontal rows of points in Fig. 2.13). Mathematically, such insensitivity is detected from the following formula for sensitivity factor α_iß56:

$$\alpha_i = \frac{\bar{X}_i}{\bar{F}}\frac{\partial F}{\partial X_i} \qquad (i = 1, 2, ...n) \qquad (2.17)$$

with

$$\frac{\partial F}{\partial X_i} \approx \frac{1}{2\Delta X_i}[F(\bar{X}_1, ..., \bar{X}_i + \Delta X_i, ...\bar{X}_n) - F(\bar{X}_1, ..., \bar{X}_i - \Delta X_i, ...\bar{X}_n)] \quad (2.18)$$
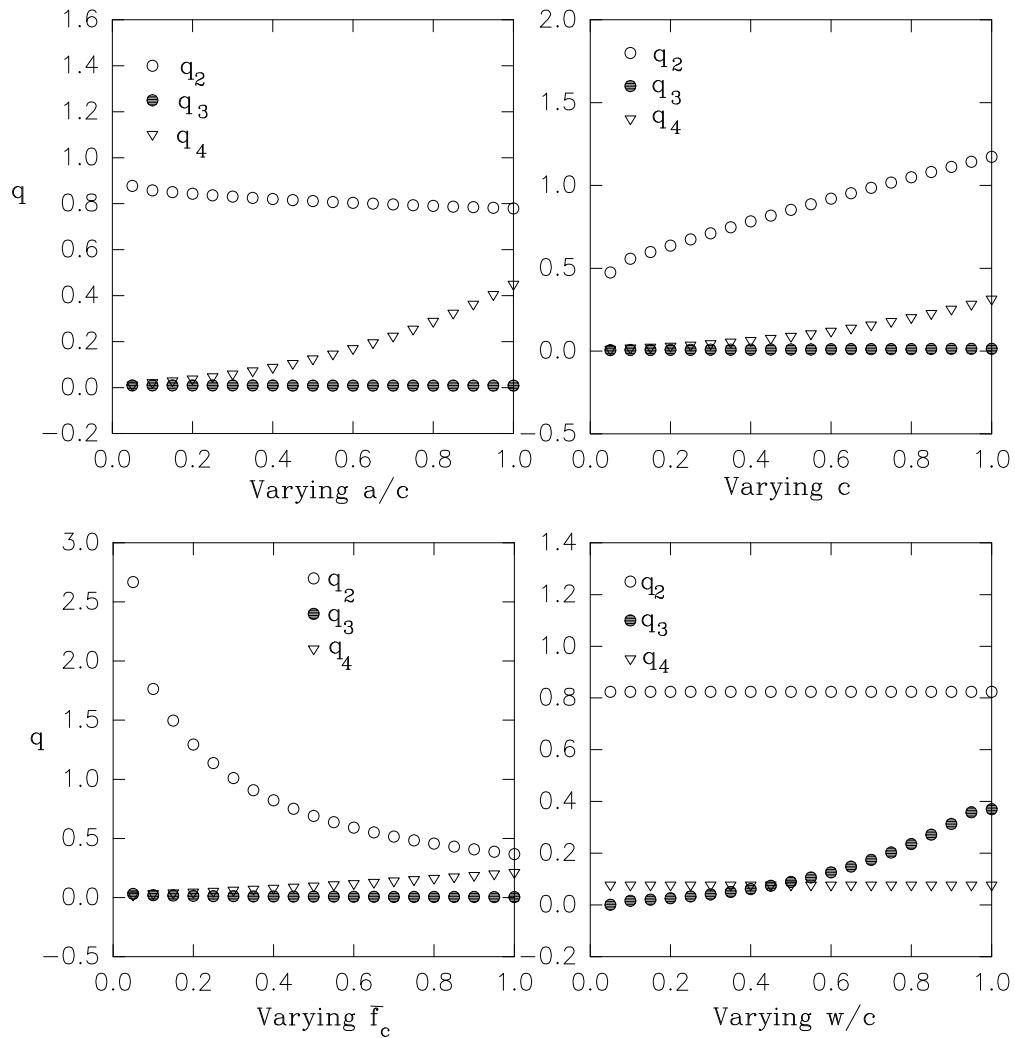
Figure 2.13: Results of the sensitivity analysis to determine important influences of composition

where F is the material property that depends upon the random parameters X_i, ΔX_i are chosen very small variations of X_i, and the superimposed bars denote the mean values. Then the composition and strength parameters to which a given model parameter is found to be insensitive are deleted from the assumed expression. The data from the data bank are then fitted again to the simplified expression and the model is optimized. If the new coefficient of variation of errors is not significantly larger the simplified expression is accepted.

It must be emphasized that the results are limited to the chosen form of dependence of model parameters on the composition and strength (products of power functions). Somewhat different trends may be found with other assumed types of dependence. Note, however, that the simplified formulae agree with general trends established by experience, experiments and considerations of physical mechanismsß57. The simplified formulae agree with the fact that creep increases with an increase in cement content and decreases

with an increase in strength and aggregate content, and that shrinkage increases with an increase in water content. The exponent 4 of w/c in Eq. (1.17) might seem too high, but it results from optimization and does not yield excessive sensitivity to w/c because q_3 is normally small compared to q_1, q_2, and q_4 (see Fig. 2.13).

In the future, the formulae for the dependence of model parameters on the basic characteristics of concrete should be based on the theory of composites. Some useful results in this regard have already been achievedß58; however no comprehensive theory for practical use is in sight at present.

Chapter 3

References

1. RILEM TC 107, "Guidelines for characterizing concrete creep and shrinkage in structural design codes or recommendations", *Materials and structures* **28** (1995), 52-55. See also RILEM TC69, "Conclusions for structural analysis and for formulation of standard design recommendations," Chapter 6 in *Mathematical Modeling of Creep and Shrinkage of Concrete*, ed. by Z.P. Bažant, John Wiley and Sons, Chichester and New York, 1988; reprinted in *Materials and Structures* (RILEM, Paris) **20** (1987), 395–398, and in *ACI Materials Journal* **84** (1987), 578–581.
2. Bažant, Z.P., and Baweja, S., "Creep and shrinkage prediction model for analysis and design of concrete structures – Model B3" Structural Engineering Report 94-10/603c, Northwestern University, (1994); Published as draft RILEM recommendation in *Materials and Structures* (RILEM Paris), **28** (1995), 357-365, 415-430, 488-495.
3. Bažant, Z.P., and Panula, L., "Practical prediction of time dependent deformations of concrete," Parts I–VI, *Materials and Structures* **11** (1978) 307–316, 317–328, 425–434, **12** (1979) 169–183.
4. Bažant, Z.P. Kim, Joong-Koo, and Panula, L., "Improved prediction model for time dependent deformations of concrete," Part 1—Shrinkage, *Materials and Structures* **24** (1991), 327–345, Part 2—Basic creep, *ibid.*, **24** 409–42, Part 3—Creep at drying, *ibid.*, **25** (1992), 21–28, Part 4—Temperature effects, *ibid.*, **25** (1992), 84–94, Part 5—Cyclic load and cyclic humidity, *ibid.*, **25** (1992) (147), 163–169.
5. "Prediction of creep, shrinkage and temperature effects in concrete structures, ACI 209 R-92," *American Concrete Institute*, Detroit 1992 (minor update of original 1972 version).
6. Bažant, Z.P., and Prasannan, S., "Solidification theory for concrete creep: I. Formulation, and II. Verification and application," *ASCE J. of Engrg. Mech.* **115** (8) (1989), 1691–1725.
7. Nasser, K.W., Al-Manaseer, A., "Creep of Concrete Containing Fly Ash and Superplasticizer at Different Stress/Strength Ratios", *American Concrete Institute Journal* **62**, (1986), 668-673.
8. Bažant, Z.P., and Liu, K.-L., "Random creep and shrinkage in structures: Sampling." *J. of Structural Engrg.*, ASCE **111** (1985), 1113–1134.

9. L'Hermite, R.G., and Mamillan M.,"Influence de la dimension des éprouvettes sur le retrait," *Ann. Inst. Techn. Bâtiment Trav. Publics* **23** (270) (1970), 5-6.

10. Crow, E.L., Davis, F.A., and Maxfield, M.W., *Statistics Manual*, Dover Publ., NewYork (1960) pp. 152–167.

11. Bažant, Z.P., and Chern, J.-C., "Bayesian Statistical Prediction of Concrete Creep and Shrinkage," *American Concrete Institute Journal* **81** (1984), 319-330.

12. Bažant, Z.P., Kim, J.-K., Wittmann, F.H., and Alou, F., "Statistical Extrapolation of Shrinkage Test Data–Part II Bayesian Updating," *ACI Materials Journal* **84** (1987), 83-91.

13. Bažant, Z.P., Xi, Y., and Baweja, S., "Improved prediction model for time dependent deformations of concrete: Part 7—Short form of BP-KX model, Statistics and extrapolation of short-time data," *Materials and Structures* **26** (1993), 567–574.

14. Granger, L., "Comportement différé du béton dans les enceintes de centrales nucléaires: analyse et modélisation", PhD thesis of ENPC, Research report of Laboratoire Central des Ponts et Chaussées, Paris, France (1995).

15. Bažant, Z.P.,"Theory of creep and shrinkage in concrete structures: A precis of recent developments," *Mechanics Today*, ed. by S. Nemat-Nasser, Pergamon Press 1975, Vol. 2 (1975) pp. 1–93.

16. Bažant, Z.P.,"Mathematical models for creep and shrinkage of concrete," Chapter 7 in *Creep and Shrinkage in Concrete Structures*, ed. by Z. P. Bažant and F. H. Wittmann, J. Wiley & Sons, London (1982), 163–256.

17. Chiorino, M.A., (Chairman of editorial team), "CEB Design Manual: Structural effects of time dependent behaviour of concrete," Georgi Publ. Co. Saint Saphorin (Switzerland) (1984), 391 pp.

18. CEB, Chiorino, M.A., Ed., *Revision of the design aids of the CEB Design Manual Structural effects of time dependent behaviour of concrete, in accordance with the CEB-FIP Model Code 1990*, Bulletin d'Information N.215 (1993) 297pp.

19. Subcommittee 7 Chaired by Z. P. Bažant. "Time dependent effects," Chap. 6 in State-of-the-Art Report on *Finite Element Analysis of Reinforced Concrete*, prepared by ASCE Str. Div. Task Committee chaired by A. Nilson, Am. Soc. of Civil Engrs., New York (1982) 309–400.

20. Bažant, Z.P., and Xi, Y., "Drying creep of concrete: Constitutive model and new experiments separating its mechanisms.", *Materials and Structures*, **27** (1994), 3–14.

21. Alvaredo, A.M., and Wittmann, F.H., "Shrinkage as influenced by strain softening and crack formation," in *Creep and Shrinkage of Concrete*, Proceedings of the 5th International RILEM Symposium, ConCreep5, Barcelona Spain (1993), 103–113.

22. Bažant, Z. P., and Chern, J.-C., "Concrete creep at variable humidity: Constitutive law and mechanism." *Materials and Structures* (RILEM,

Paris), **18** (1985), 1–20.

23. McDonald, D.B., and Roper, H., "Prediction of drying shrinkage of concrete from internal humidities and finite element techniques," in *Creep and Shrinkage of Concrete*, Proceedings of the 5th International RILEM Symposium, ConCreep 5, Barcelona Spain (1993), 259–264.

24. Bažant, Z.P., and Kim, S.S., "Approximate relaxation function for concrete," *Journal of the Structural Division, ASCE*, **105** (1979), 2695–2705.

25. Bažant, Z.P., "Prediction of concrete creep effects using age-adjusted effective modulus method," *American Concrete Institute Journal* **69** (1972), 212–217.

26. *Mathematical modeling of creep and shrinkage of concrete*, ed. by Z.P. Bažant, John Wiley & Sons, Chichester and NewYork (1988).

27. Bažant, Z. P., and Osman, E., "Double power law for basic creep of concrete." *Materials and Structures (RILEM, Paris)*, **9** (1976), 3–11.

28. Brooks, J.J., "Preliminary state of the art report: Elasticity, creep and shrinkage of concretes containing admixtures, slag, fly-ash and silica-fume" *Preliminary Report* ACI committee 209 (1992).

29. Brooks, J.J., "Influence of mix proportions, plasticizers and superplasticizers on creep and drying shrinkage of concrete," *Magazine of concrete research* **41**(148) (1989), 145-153.

30. CEB-FIP Model Code (1990), Design Code, Thomas Telford, London.

31. Gardner, N.J., and Zhao, J.W., "Creep and shrinkage revisited," *ACI Materials Journal* **90** (1993) 236-246. Discussion by Bažant and Baweja, *ACI Materials Journal* **91** (1994), 204-216.

32. Keeton, J.R., "Study of creep in concrete, *Technical reports* R333-I, R333-II, R333-III," U.S. Naval civil engineering laboratory, Port Hueneme, California (1965).

33. Wallo, E.M., Yuan, R.L., Lott, J.L., Kesler, C.E., "Sixth progress report on prediction of creep in structural concrete from short time tests". *T & AM Report* No. 658, Department of Theoretical and Applied Mechanics, University of Illinois at Urbana (1965).

34. L'Hermite, R.G., and Mamillan M.,"Influence de la dimension des éprouvettes sur le retrait," *Ann. Inst. Techn. Bâtiment Trav. Publics* **23** (270) (1970), 5-6.

35. L'Hermite, R.G., Mamillan, M. Lefèvre, C., "Nouveaux résultats de recherches sur la déformation ét la rupture du béton," *Ann. Inst. Techn. Bâtiment Trav. Publics* **18** (207-208), (1965), 323-360.

36. Wittmann, F.H., Bažant, Z.P., Alou, F., Kim, J.K., "Statistics of shrinkage test data," *Cem., Conc. Aggreg.* ASTM **9**(2) (1987) 129-153.

37. Kommendant, G.J., Polivka, M., and Pirtz, D., *Study of concrete properties for prestressed concrete reactor vessels*, Final Report No. UC-SESM 76-3 (to General Atomic Company), Department of Civil Engineering, University of California, Berkeley (1976).

38. Rostasy, F.S., Teichen, K.-Th. and Engelke, H., "Beitrag zur Klärung des Zussammenhanges von Kriechen und Relaxation bei Normal-beton," Amtliche Forschungs-und Materialprüfungsanstalt für das Bauwesen,

Heft 139 (Otto-Graf-Institut, Universität Stuttgart, (Strassenbau-und Strassenverkehrstechnik) (1972).

39. Hansen, T.C., and Mattock, A.H., "Influence of size and shape of member on the shrinkage and creep of concrete," *ACI J.* **63**, (1966), 267-290.

40. Troxell, G.E., Raphael, J.E. and Davis, R.W., "Long-time creep and shrinkage tests of plain and reinforced concrete," *Proc. ASTM* **58** (1958), 1101-1120.

41. Russell, H., and Burg, R., Test data on Water Tower Place Concrete from Russell, H.G., and Fiorato, A.E., "High strength concrete research for buildings and bridges", ACI SP-159, to be published.

42. Browne, R.D., "Properties of concrete in reactor vessels," in *Proc. Conference on Prestressed Concrete Pressure Vessels* Group C Institution of Civil Engineers, London (1967) pp. 11-31.

43. Hannant, D.J., "Strain behaviour of concrete up to 95°C under compressive stresses" in *Proc. Conference on Prestressed Concrete Pressure Vessels* Group C, Institution of Civil Engineers, London (1967) pp. 57-71.

44. Takahashi, H., Kawaguchi, T. "Study on time-dependent behaviour of high-strength concrete (Part 1)–Application of the Time-Dependent Linear Viscoelasticity Theory of Concrete Creep Behaviour," Report No 21, Ohbayashi-Gumi Research Institute, Tokyo (1980), pp. 61-69.

45. Shideler J.J. "Lightweight aggregate concrete for structural use," *ACI Journal* (1957), 299–328.

46. Taylor, H.F.W., *Cement chemistry*, Academic Press, London (1990).

47. Hansen, W., "Drying shrinkage mechanisms in Portland cement pastes," *J. Am. Ceram. Soc.* **70**, 5, 323–328 (1987).

48. Xi, Y., Bažant, Z.P., and Jennings, H.M., "Moisture diffusion in cementitious materials: Adsorption Isotherms" *J. Adv. Cement Based Mater.* **1** (6) (1994).

49. Powers, T.C., and Brownyard, T.L. *Proc. ACI* (1946-47) 43, 101, 149, 469, 549, 845, 933.

50. Bažant, Z.P., and Kim, Joong-Koo., "Consequences of diffusion theory for shrinkage of concrete" *Materials and Structures* **24** (1991), 323-326.

51. de Larrard, F., Acker, P., and LeRoy, R., "Shrinkage creep and thermal properties," chapter 3 in *High performance concrete and applications*, S.P. Shah and S.H. Ahmad, Eds., Edward Arnold, London (1994).

52. Carol, I., and Bažant, Z.P., "Viscoelasticity with aging caused by solidification of non aging constituent." *ASCE J. of Engg. Mech.* **119** (11) (1993) 2252-2269.

53. Bažant, Z.P., Şener, S., and Kim, Jenn-Keun, "Effect of cracking on drying permeability and diffusivity of concrete.," *ACI Materials Journal*, **84** (Sept.-Oct.), 351–357 (1987).

54. Mandel, J., *The statistical analysis of experimental data*, J. Wiley–Interscience, NewYork (1964).

55. Crow, E.L., Davis, F.A., and Maxfield, M.W., *Statistics Manual*, Dover Publ., NewYork (1960) pp. 152–167.

56. Tsubaki, T., "Sensitivity of factors in relation to prediction of creep and shrinkage of concrete" in *Creep and Shrinkage of Concrete*, Proceedings of 5th International RILEM Symposium (ConCreep 5), Barcelona, Spain (1993), 611-622.

57. Neville, A.M., Dilger, W.H. and Brooks, J.J., *Creep of plain and structural concrete*, Construction Press, London and NewYork (1983).

58. Granger, L., and Bažant, Z.P. "Effect of composition on basic creep of concrete" (1993) Structural Engineering Report No. 93-8/603e Northwestern University Evanston, Illinois.

Figure A1. Unrealistic and theoretically unfounded shapes of typical shrinkage curves of GZ model (h = enviromnental humidity, $t - t_0$ = duration of drying).

Figure A2. Unrealistic and theoretically objectionable reversals of creep recovery curves obtained from the GZ model (top) and the CEB-FIP model (bottom) according to the principle of superposion.

Figure A3. Stress relaxation curves obtained from the GZ model (top) and the CEB-FIP model (bottom) according to the principle of superposition (the fact that these curves cross the horizontal axis and reach into opposite stress values is unrealistic and theoretically questionable)

Figure A3–Continuation. Stress relaxation curves obtained according to the principle of superposition from the present B3 model (it has been mathematically proven that these curves can never cross the horizontal axis and reach into opposite stress values).

3.1 Comparison with Gardner and Zhao's (GZ) Model and Other Models

To further justify the present model, it is desirable to clarify the differences from other models, and especially from the GZ Modelß31, which is also presented in this volume. The following comparison summarizes the contents of a recent detailed critical discussion of this modelß31.

The statistical comparisons of the data points presented by the proponents of the GZ Model were limited. If comparisons with all the significant test data available are made, a clearer picture of the predictive capability of the model can be seen. Some comparisons were already listed in the aforementioned discussionß31.

Furthermore, many basic features of Model GZ are questionable on the basis of the current understanding of the mechanics and physics of concrete shrinkage and creep, and violate the guidelines recently published by a RILEM Committeeß1. These are as follows:

1. *Lack of bounded final shrinkage:* The shrinkage curve for Model GZ does not have a final asymptotic value (Fig. A1). Although most test data have been obtained on specimens too thick to dry up completely and approach the final shrinkage value, the relevant tests on thinner specimens which did dry up completely clearly confirm that a bounded final value exists. Furthermore, the existing and generally accepted theory of the shrinkage mechanism requires a bounded final shrinkage value to exist (see, e.g., the state-of-the-art review in Chapter 1 of Mathematical Modeling, 1988, J. Wiley). Briefly, the reason is the finiteness of the values of the capillary forces and adsorption film forces that can be produced by drying, and the finiteness of the value of water that can be withdrawn from concrete. Also, the physical-chemical processes that cause drying are known to cease after the evaporable water has escaped from concrete. The shrinkage curve of the GZ model terminates with an inclined straight line in $\log (t - t_0)$, which has been based on the data of Troxell et al.ß40. However these data obtained on a 1930's type low quality concrete are an anomaly. No other data in the RILEM data bank support such a final asymptote of the shrinkage curve.

by drying, and the finiteness of the value of water that can be withdrawn from concrete. Also, the physical-chemical processes that cause drying are known to cease after the evaporable water has escaped from concrete. The shrinkage curve of the GZ model terminates with an inclined straight line in $\log(t - t_0)$, which has been based on the data of Troxell et al.ß40 However these data obtained on a 1930's type low quality concrete are an anomaly. No other data in the RILEM data bank support such a final asymptote of the shrinkage curve.

2. *Disagreement with diffusion theory:* The generally accepted nonlinear diffusion theory for drying and shrinkage requires that the initial portion of the shrinkage curve should evolve in proportion to the $\sqrt{(t - t_0)/D^2}$, where $t - t_0$ = duration of drying and D = effective thickness of the specimen. This property is violated by Model GZ but not by Model B3.

3. *Negative initial shrinkage:* The shrinkage should always be positive, as exhibited by the B3 and other models, but violated by Model GZ. Although this violation exists only for very short times (less than 1 min.), this is in principle incorrect. It is of course true that some shrinkage tests indicate negative initial shrinkage, but this is due to hydration heat and crystal growth pressure in very thick specimens. Without taking these phenomena into account by special parameters, it is not correct to use a formula that exhibits negative initial shrinkage in all the situations.

4. *Characterizing the age effect by strength gain*: The effect of age on creep according to Model GZ is far too weak and too short-lived. This is due to relating this effect to the age affect on concrete strength. It is known that the increase of concrete strength with the age ceases after about one year, but the effect of age on concrete creep continues for many years. This is due to basic differences in the mechanisms (especially the fact that long-term aging is due to exhaustion of the creep sites and to relaxation of the microprestress in the microstructure, rather than to the chemical reaction of hydration).

5. *Lack of final value of drying creep:* The creep coefficient for the additional creep due to drying is given in Model GZ by a curve that does not have a bounded final value. This is incorrect for the same reasons as stated for shrinkage

6. *Unsuitability for computer analysis of structures:* For computer analysis of structures, it is a major advantage if the compliance function of the model can be easily converted into a rate-type constitutive relation based on the Maxwell chain or Kelvin chain. For the Model B3, this conversion is automatic because there exists a simple and explicit formula to accomplish it. For the form of Model GZ, such an explicit formula does not exist, and cumbersome nonlinear fitting by the rate-type model is required for that purpose.

7. *Linearity with respect to the basic parameters*: Often the user may have test data on his concrete. Then it is important for the model to have the capability of easy adjustment to fit such limited test data. The adjustment is easy and unambiguous only if the main parameters of the model are involved in the formulas linearly. This is true of the basic parameters of the B3 Model (parameters q_0, q_1, q_2, q_3, q_4, q_5) but not of the parameters of the Model GZ. This means that linear regression cannot be used to adjust the GZ model to the given data.

8. *Extrapolation based on given short-time data*: For creep sensitive structure, the user should conduct short-time tests of 1 to 6 months duration, and then adjust the model to fit these short-time tests, thus obtaining an extrapolation of the short-time tests into long times. Simple procedures for adjusting the B3 Model to short time data for creep or shrinkage have been worked out, but they are unavailable for the Model GZ.

9. *Non-monotonic creep recovery (recovery reversal)*: The creep recovery curve calculated according to the principle of superposition must descend monotonically, i.e. must not reverse to a rising curve. This property is verified by the B3 model, both for basic creep and creep at drying but is violated by the GZ model (Fig. A2 (a,b)). Such behavior is, according to the solidification theory, thermodynamically inadmissible.

10. *Stress relaxation curves with a change of stress sign*: The stress relaxation curves calculated from GZ model using principle of superposition exhibit a change of stress sign. Such curves are thermodynamically inadmissible and they do not arise for Model B3 for both basic creep and creep at drying as demonstrated in Fig. A3 (a,b).

11. *Negative or decreasing elastic moduli and viscosities of Kelvin chain approximation*: Large-scale finite element analysis for creep requires that the compliance function be approximated by a Kelvin Chain consisting of springs and dashpots. When the solidification theory is not followed (e.g. when the creep recovery exhibits a reversal or the relaxation curve changes its sign), the spring moduli and the dashpot viscosities are obtained as negative for some periods of time, and may decrease in time, both of which are inadmissible and cause convergence problems. For the B3 model this can-not happen, but it does for the GZ model.

The typical shrinkage curves according to the GZ model are shown in Fig. A1(a). Comparison with Fig. 1.1 for the B3 model reveals great differences. For the reasons just mentioned, the shapes of these curves are not very realistic and, on the average, do not allow good fits of the individual measured creep curves. Of course, in comparison to a set of many test data, this is often obscured by the large scatter.

Since the CEB-FIP modelß30 has not been under consideration by the ACI committee 209, its limitations will be pointed out only tersely. This

model, which incorporated many features of the BP Model and was one of the best when developed in the mid 1980's does not satisfy the RILEM guidelines No. 2, 8, 9, 10, 11, 12, 13, 15, 20 and 21 and partly also 6 and 7. It does not follow the solidification theory (it was formulated earlier than that theory), and consequently it exhibits problems of recovery reversal and change of stress sign for stress relaxation; see Fig. A2(c), A3(c). The leveling off of the basic creep curves in $\log (t - t')$ scale after several years of loading and the fact that a finite asymptotic value of creep is assumed is not justified and may result in underestimation of long term creep. Some features of the shrinkage formulation do not follow the diffusion theory (absence of shape effect, approach to final value), and the formulation for additional creep due to drying is completely empirical.

Addendum:

4.1 Comparison with Gardner and Zhao's (GZ) Model and Other Models

To further justify the present model, it is desirable to clarify the differences from other models, and especially from the GZ Model[31], which is also presented in this volume. The following comparison summarizes the contents of a recent detailed critical discussion of this model[31].

The statistical comparisons of the data points presented by the proponents of the GZ Model were limited. If comparisons with all the significant test data available are made, a clearer picture of the predictive capability of the model can be seen. Some comparisons were already listed in the aforementioned discussion[31].

Furthermore, many basic features of Model GZ are questionable on the basis of the current understanding of the mechanics and physics of concrete shrinkage and creep, and violate the guidelines recently published by a RILEM Committee[1] . These are as follows:

1. *Lack of bounded final shrinkage:* The shrinkage curve for Model GZ does not have a final asymptotic value (Fig. A1). Although most test data have been obtained on specimens too thick to dry up completely and approach the final shrinkage value, the relevant tests on thinner specimens which did dry up completely clearly confirm that a bounded final value exists. Furthermore, the existing and generally accepted theory of the shrinkage mechanism requires a bounded final shrinkage value to exist (see, e.g., the state-of-the-art review in Chapter 1 of Mathematical Modeling, 1988, J. Wiley). Briefly, the reason is the finiteness of the values of the capillary forces and adsorption film forces that can be produced by drying, and the finiteness of the value of water
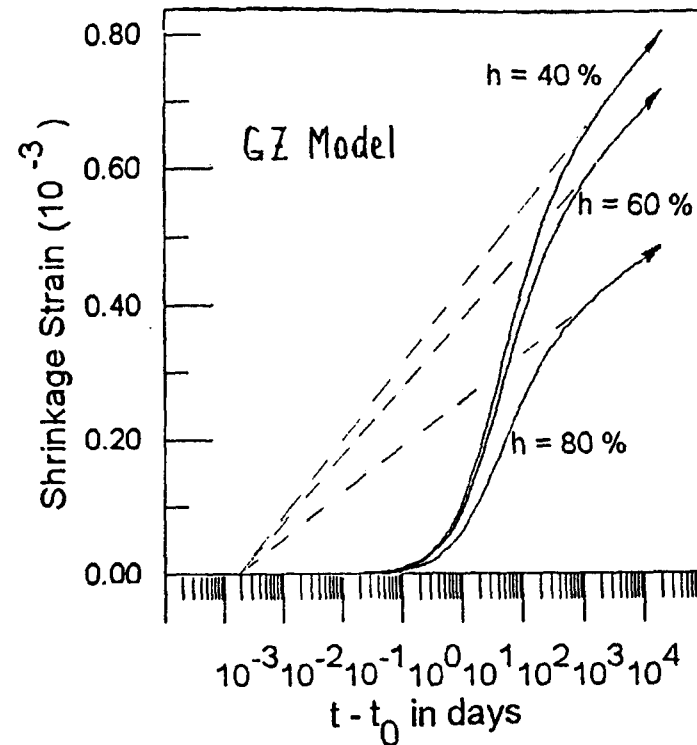

Figure A1. Unrealistic and theoretically unfounded shapes of typical shrinkage curves of GZ model (h = environmental humidity, $t - t_0$ = duration of drying).

that can be withdrawn from concrete. Also, the physical-chemical processes that cause drying are known to cease after the evaporable water has escaped from concrete. The shrinkage curve of the GZ model terminates with an inclined straight line in log $(t - t_0)$, which has been based on the data of Troxell et al.[40] However these data obtained on a 1930's type low quality concrete are an anomaly. No other data in the RILEM data bank support such a final asymptote of the shrinkage curve.

2. *Disagreement with diffusion theory:* The generally accepted nonlinear diffusion theory for drying and shrinkage requires that the initial portion of the shrinkage curve should evolve in proportion to the $\sqrt{(t - t_0)/D^2}$, where $t - t_0$ = duration of drying and D = effective thickness of the specimen. This property is violated by Model GZ but not by Model B3.

3. *Negative initial shrinkage:* The shrinkage should always be positive, as exhibited by the B3 and other models, but violated by Model GZ. Although this violation exists only for very short times (less than 1 min.), this is in principle incorrect. It is of course true that some shrinkage tests indicate negative initial shrinkage, but this is due to hydration heat and crystal growth pressure in very thick specimens. Without taking these phenomena into account by special parameters, it is not correct to use a formula that exhibits negative initial shrinkage in all the situations.

4. *Characterizing the age effect by strength gain:* The effect of age on creep according to Model GZ is far too weak and too short-lived. This is due to relating this effect to the age affect on concrete strength. It is known that the increase of concrete strength with the age ceases after about one year, but the effect of age on concrete creep continues for many years. This is due to basic differences in the mechanisms (especially the fact that long-term aging is due to exhaustion of the creep sites and to relaxation of the microprestress in the microstructure, rather than to the chemical reaction of hydration).

5. *Lack of final value of drying creep:* The creep coefficient for the additional creep due to drying is given in Model GZ by a curve that does not have a bounded final value. This is incorrect for the same reasons as stated for shrinkage
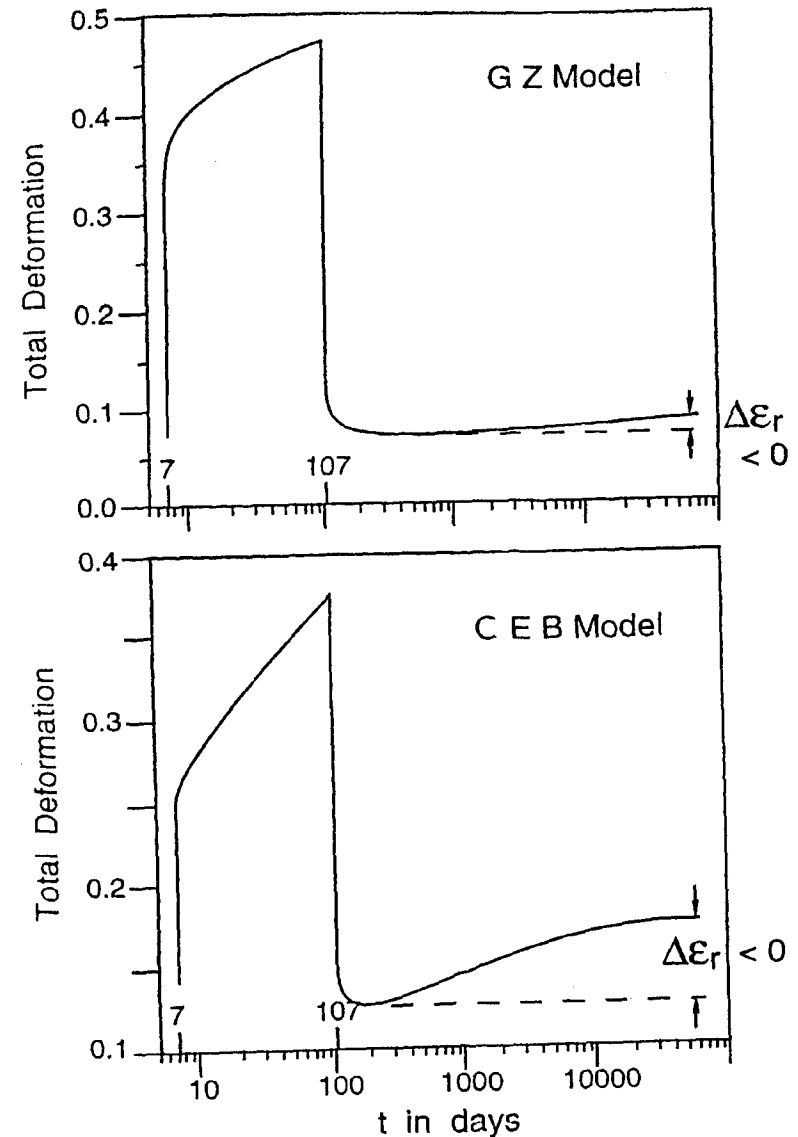

Figure A2. Unrealistic and theoretically objectionable reversals of creep recovery curves obtained from the GZ model (top) and the CEB-FIP model (bottom) according to the principle of superposition.

6. *Unsuitability for computer analysis of structures:* For computer analysis of structures, it is a major advantage if the compliance function of the model can be easily converted into a rate-type constitutive relation based on the Maxwell chain or Kelvin chain. For the Model B3, this conversion is automatic because there exists a simple and explicit formula to accomplish it. For the form of Model GZ, such an explicit formula does not exist, and cumbersome nonlinear fitting by the rate-type model is required for that purpose.

7. *Linearity with respect to the basic parameters:* Often the user may have test data on his concrete. Then it is important for the model to have the capability of easy adjustment to fit such limited test data. The adjustment is easy and unambiguous only if the main parameters of the model are involved in the formulas linearly. This is true of the basic parameters of the B3 Model (parameters q_0, q_1, q_2, q_3, q_4, q_5) but not of the parameters of the Model GZ. This means that linear regression cannot be used to adjust the GZ model to the given data.

8. *Extrapolation based on given short-time data:* For creep sensitive structure, the user should conduct short-time tests of 1 to 6 months duration, and then adjust the model to fit these short-time tests, thus obtaining an extrapolation of the short-time tests into long times. Simple procedures for adjusting the B3 Model to short time data for creep or shrinkage have been worked out, but they are unavailable for the Model GZ.

9. *Non-monotonic creep recovery (recovery reversal):* The creep recovery curve calculated according to the principle of superposition must descend monotonically, i.e. must not reverse to a rising curve. This property is verified by the B3 model, both for basic creep and creep at drying but is violated by the GZ model (Fig A2 (a,b)). Such behavior is, according to the solidification theory, thermodynamically inadmissible.

10. *Stress relaxation curves with a change of stress sign:* The stress relaxation curves calculated from GZ model using principle of superposition exhibit a change of stress sign. Such curves are thermodynamically inadmissible and they do not arise for Model B3 for both basic creep and creep at drying as demonstrated in Fig A3 (a,b).

11. *Negative or decreasing elastic moduli and viscosities of Kelvin chain approximation:* Large-scale finite element analysis for creep requires that
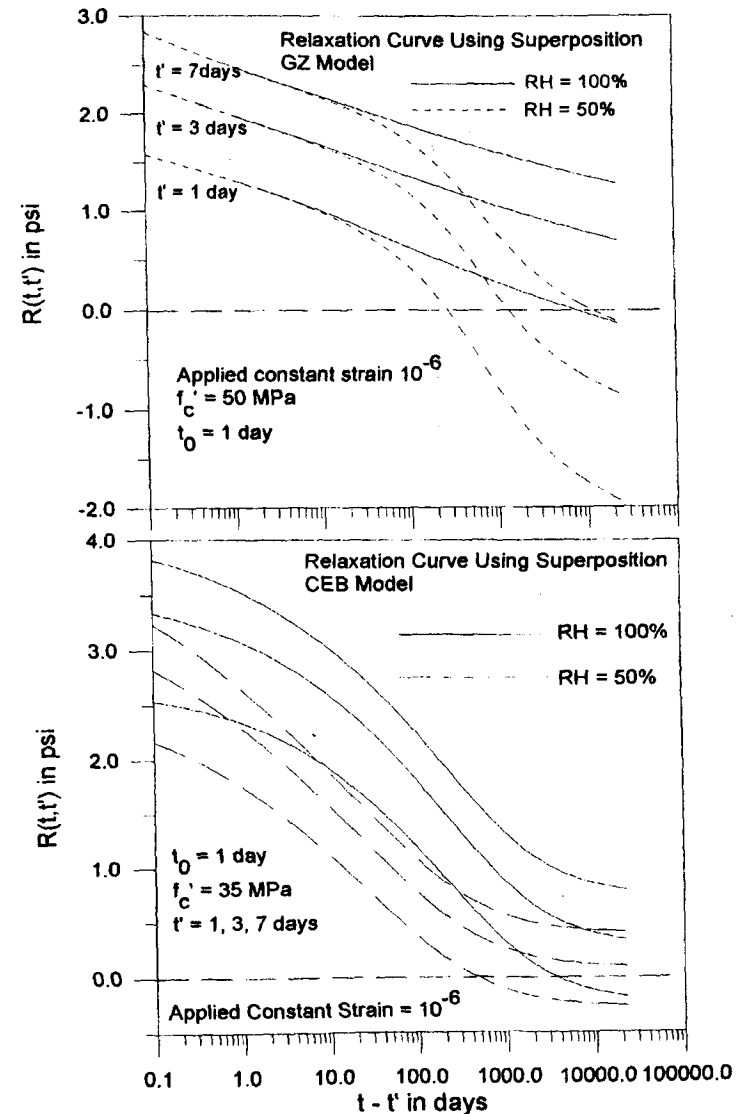

Figure A3. Stress relaxation curves obtained from the GZ model (top) and the CEB-FIP model (bottom) according to the principle of superposition (the fact that these curves cross the horizontal axis and reach into opposite stress values is unrealistic and theoretically questionable).
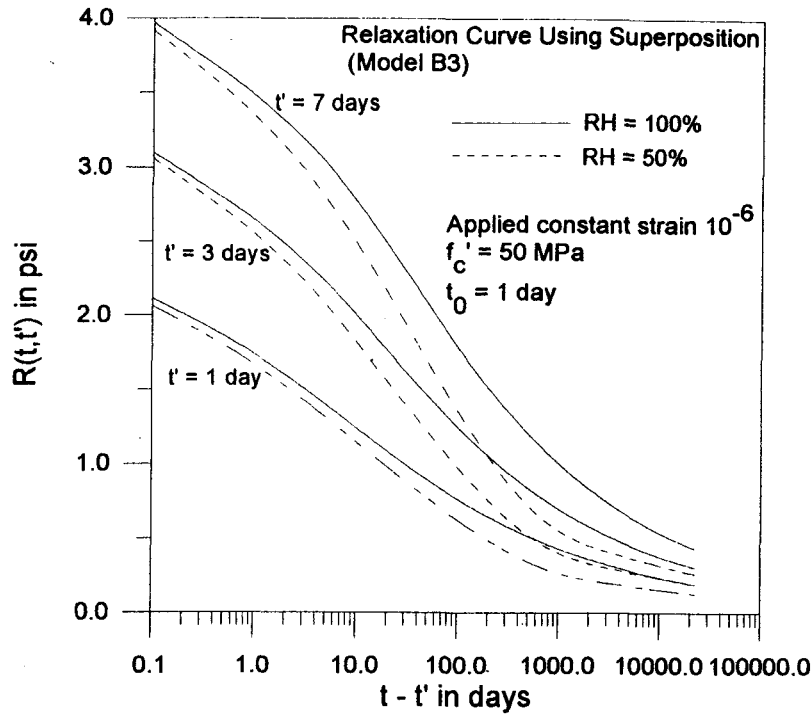
Figure A3–Continuation. Stress relaxation curves obtained according to the principle of superposition from the present B3 model (it has been mathematically proven that these curves can never cross the horizontal axis and reach into opposite stress values).

the compliance function be approximated by a Kelvin Chain consisting of springs and dashpots. When the solidification theory is not followed (e.g. when the creep recovery exhibits a reversal or the relaxation curve changes its sign), the spring moduli and the dashpot viscosities are obtained as negative for some periods of time, and may decrease in time, both of which are inadmissible and cause convergence problems. For the B3 model this can-not happen, but it does for the GZ model.

The typical shrinkage curves according to the GZ model are shown in Fig. A1(a). Comparison with Fig. 1.1 for the B3 model reveals great differences. For the reasons just mentioned, the shapes of these curves are not very realistic and, on the average, do not allow good fits of the individual measured creep curves. Of course, in comparison to a set of many test data, this is often obscured by the large scatter.

Since the CEB-FIP model[30] has not been under consideration by the ACI committee 209, its limitations will be pointed out only tersely. This model, which incorporated many features of the BP Model and was one of the best when developed in the mid 1980's does not satisfy the RILEM guidelines No. 2, 8, 9, 10, 11, 12, 13, 15, 20 and 21 and partly also 6 and 7. It does not follow the solidification theory (it was formulated earlier than that theory), and consequently it exhibits problems of recovery reversal and change of stress sign for stress relaxation; see Fig. A2(c), A3(c). The leveling off of the basic creep curves in log $(t - t')$ scale after several years of loading and the fact that a finite asymptotic value of creep is assumed is not justified and may result in underestimation of long term creep. Some features of the shrinkage formulation do not follow the diffusion theory (absence of shape effect, approach to final value), and the formulation for additional creep due to drying is completely empirical.

The coefficients of variation of the errors of various models have been calculated, as already described in Sec. 2.2. For convenience, they are now summarized in Table A1. This calculation was based on the 1996 version of the RILEM data bank (this version did not include several data sets added subsequently, but it was checked that the addition of these data sets did not change the statistics significantly).

Table A1. Coefficients of variation of prediction errors.

Model	B3	ACI	GZ	CEB-90
Shrinkage	34	55	48	46
Basic creep	24	58	46	35
Drying creep	23	45	38	32